

Computation of Stabilizing and Relatively Optimal Feedback Control Laws Based on Demonstrations

Jiří Fejlek^{1,2*} and Stefan Ratschan^{1†}

¹The Czech Academy of Sciences, Institute of Computer Science

²Czech Technical University in Prague, Faculty of Nuclear Sciences and Physical Engineering

February 28, 2022

Abstract

Assume a demonstrator that for any given state of a control system produces control input that steers the system toward the equilibrium. In this paper, we present an algorithm that uses such a demonstrator to compute a feedback control law that steers the system toward the equilibrium from any given state, and that, in addition, inherits optimality guarantees from the demonstrator. The resulting feedback control law is based on switched LQR tracking, and hence the resulting controller is much simpler and allows for a much more efficient implementation than a control law based on the direct usage of a typical demonstrator. Our algorithm is inspired by techniques from robot motion planning such as simulation based LQR trees, but also produces a Lyapunov-like function that provides a certificate for the stability of the resulting controller. And moreover, we provide rigorous convergence and optimality results for the convergence of the algorithm itself.

1 Introduction

This paper addresses the feedback motion planning problem by providing an algorithm that for every given system of ordinary differential equations with control inputs synthesizes a controller that asymptotically stabilizes the system on some given compact set that contains the equilibrium. Assuming that some cost is assigned to control, we additionally aim at minimization of this cost.

An important method for controller design uses the knowledge of a suitable control-Lyapunov function (CLF) [40]. From a CLF, a stabilizing controller can be given explicitly for control-affine systems using universal formulas [39, 13]. However, the resulting controller usually does not take into account any cost [15], even when the CLF was constructed using demonstrations that meet them [34]. Another drawback to consider is the fact, that the resulting controller is properly defined only on some sublevel set of the CLF that is fully contained in the set where the CLF was constructed. This sublevel set can be significantly smaller than the whole investigated set, leaving the rest to waste.

To alleviate the drawbacks of the construction of stabilizing controllers based on CLFs alone, we propose a natural extension of learning CLF from demonstrations [34] to learning a stabilizing controller from demonstrations, as well. If the demonstrator minimizes cost, the learned controller also inherits this property, at least asymptotically for an increasing number of demonstrations. We introduce a generic algorithm, and investigate more closely its instantiation with a controller based on LQR tracking [43, 36]. Based on this, we propose a novel LQR switching controller whose stability is verified using the learned CLF on the whole investigated set, hence also dealing with the problem of sublevel sets. We also do computational experiments on several examples of dimension up to twelve that demonstrate the practical applicability of the method. We compare the performance of the resulting controllers with the ones resulting from Sontag's universal formula [39] and the run-time of the algorithm with an approach based fully on system simulations [36] (i.e. with no Lyapunov function learning). We demonstrate that the performance of the controllers constructed by our method is indeed better (between 10 and 50 percent) and that time savings are significant (at least 50 percent on average).

*ORCID: 0000-0002-9498-3460

†ORCID: 0000-0003-1710-1513

The structure of the paper is as follows. In Section 2, we state the precise problem and discuss related work. In Section 3, we introduce a general layout of our algorithm. In Section 4, we concretize the general idea into a controller based on LQR tracking and explore its theoretical properties. We expand this topic further in Section 5, where we describe the implementation itself. In Section 6 we provide the computational experiments. And finally, Sections 7 and 8 contain a discussion and a conclusion. Proofs of all propositions are included in the appendix.

This work was funded by institutional support of the Institute of Computer Science (RVO:67985807).

2 Problem Statement and Related Work

Consider a control system of the form

$$\dot{x} = F(x, u) \quad (1)$$

where $F: \mathbb{R}^n \times \mathbb{R}^m \mapsto \mathbb{R}^n$ is a smooth function. We assume that the system has a unique solution for any initial point x_0 and control input $u: [0, \infty] \rightarrow \mathbb{R}^m$. We denote this solution by $\Sigma(x_0, u)$, which is a function in $[0, \infty] \rightarrow \mathbb{R}^n$. We also use the same notation to denote the solution of the closed loop system resulting from a feedback control law $u: \mathbb{R}^n \times [0, \infty] \rightarrow \mathbb{R}^m$. For any cost functional $V(x, u)$, where u can again be either open loop control input or a feedback control law, we denote by $\text{cost}_V(x_0, u)$ the cost of the solution $\Sigma(x_0, u)$ and its corresponding control input (i.e., u itself, if it is an open loop control input, and $u': [0, \infty] \rightarrow \mathbb{R}^m$ with $u'(t) = u(\Sigma(x_0, u)(t), t)$, if u is a feedback control law).

Let $\bar{x} = 0$ be the desired equilibrium point of the system (1), $F(0) = 0$, and $D \subseteq \mathbb{R}^n$ our region of interest that is compact, and contains the equilibrium. We also assume an $\epsilon_0 > 0$ together with an asymptotically stabilizing controller on an ϵ_0 -neighbourhood H^{ϵ_0} of the equilibrium, with H^{ϵ_0} in the interior of D . Such a controller can, for example, be obtained using linearization of the system dynamics around the equilibrium (if this linearization is asymptotically stabilizable) and solving the appropriate algebraic Riccati equation [25].

Our goal is to construct a feedback control law $u: \mathbb{R}^n \times [0, \infty] \rightarrow \mathbb{R}^m$ such that

- the resulting closed loop system $\dot{x}(t) = F(x(t), u(x, t))$ is *asymptotically stable on D* in the sense that for every $x_0 \in D$, $\lim_{t \rightarrow +\infty} \Sigma(x_0, u)(t) = 0$, and that
- for every $x_0 \in D$, $\text{cost}_V(x_0, u)$ is minimal for the cost functional

$$V(x, u) := \int_0^{+\infty} Q(x(t)) + R(u(x(t), t)) dt. \quad (2)$$

where $Q: \mathbb{R}^n \mapsto \mathbb{R}$ and $R: \mathbb{R}^m \mapsto \mathbb{R}$ are both smooth and positive definite.

Note that our presented approach does not inherently require the performance to be measured in terms of (2). However, finite cost (2) necessarily implies asymptotic stability of the system, making the tasks stabilization and optimization compatible and not conflicting.

In the control-affine case, any smooth control-Lyapunov function [38, 40] provides an explicit formula for a feedback control law for system (1) which is usually called Sontag's universal formula [39]. An alternative universal formula is a min-norm formula [13, 14] which is inverse optimal (optimal according to some meaningful cost) [37]. Unfortunately, if we fix a cost functional beforehand, there is no straightforward way how to choose a suitable formula. Moreover, there is generally no way to express the cost of the control law as an explicit function of parameters of the formula other than solving the corresponding generalized Hamilton-Jacobi-Bellman equation [7]. To address this issue, we construct a suitable CLF and a control law together.

Our approach is based on the concept of learning from demonstrations, which is well known in robotics [35]. Learning a CLF from demonstrations already has been shown to be an attractive alternative to the SOS method [41] for finding a CLF [34]. Here, one can restrict the search for a CLF to candidates that are compatible with the given demonstrations [45, 21, 34]. But a demonstrator can also provide trajectories of exemplary performance in terms of cost (2). Hence, we use these trajectories to also learn a high-performance control law [36, 43]. Note however, that we do *not* require the demonstrator to provide optimal performance. Hence, our performance guarantees will only be *relative* to the performance guarantees of the demonstrator.

Still, having a CLF and not just a set of exemplary trajectories eliminates the need to simulate whole system trajectories to check stability [36] or to investigate stability of each individual trajectory tracking system separately [43]. We also simplify the approach [36, 43] by removing explicit estimation of control funnels, i.e. sets of points for which a constructed control law based on a chosen exemplary trajectory stabilizes the system. We will just assume that these trajectories are for each point chosen via some mapping. Such a

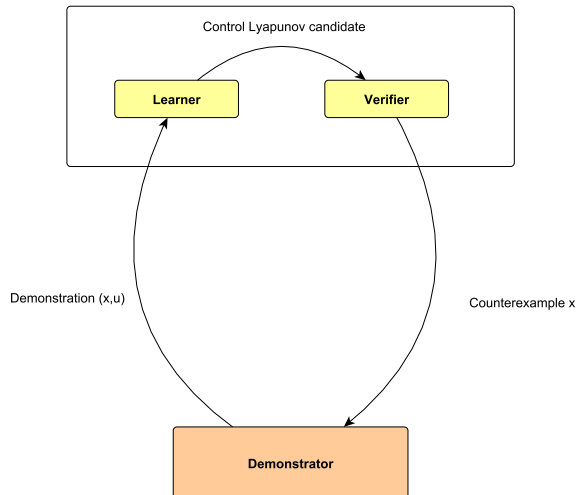


Figure 1: Overview of the learning algorithm for finding a CLF.

mapping defines approximations of control funnels only implicitly and moreover, all points from the region of interest D are in some control funnel by definition. Hence, it alleviates the problem of covering the whole region by aforementioned control funnels [36, 43]. It should be also noted that we explore the theoretical properties of the resulting algorithm more deeply and hence obtain stronger results for its successful construction of stabilizing control law on D , namely after finitely many iterations versus its construction only in the limit for the number of iterations tending to infinity [36, 43].

The usage of trajectory optimization for synthesizing feedback control laws is not new [27]. However, the resulting control laws are usually based on neural networks, whose precise behavior is difficult to understand and verify. This problem has been partially solved by recent approaches [12, 1] that use SMT (satisfiability modulo theories) solvers [6] for verification. Indeed, it is possible to apply such formal verification techniques also to the control laws synthesized by our method. However, in contrast to techniques based on neural networks, we also have rigorous convergence proofs for our algorithms.

We will now describe the results in [34] in greater detail, since the approach (see Figure 1) using a combination of a demonstrator (that provides demonstration for learning) and a verifier/falsifier (that provides counterexamples) is integral to our approach. First, let us assume a demonstrator that generates stabilizing open-loop control laws. Such a demonstrator could, for example be based on trajectory optimization [9] or planning [23, 30]. Then a set $\{L_p(x) \mid p \in P\}$ of a linearly parametrized system of functions is considered, where $P = [p_{\min}, p_{\max}]^d$, and it is supposed that $L_p(x)$ can be a CLF for the investigated system for some values of the parameters p . Suitable values for those parameters are determined by generating ordered pairs (x, u) provided by the demonstrator and finding parameters p that represent a candidate $L_p(x)$ that is strictly positive on those demonstrations, but whose value decreases along them. For a linearly parametrized system, these conditions translate to a system of linear inequalities for parameters p and all solutions will lie in some polyhedron contained in P . The candidate is chosen as a centre of the maximum volume ellipsoid [34]. It can be shown that finding the centre is a convex optimization problem [10]. The reason for this particular choice is the fact that the volume of the admissible set after adding a new constraint due to a new demonstration (assume we have not found a CLF) is decreases with a linear convergence rate [34, 42]. As soon as a candidate has been chosen, a verifier based on semidefinite programming is used to check the validity of the CLF conditions and to provide counterexamples for further learning. Adding more and more counterexamples, the algorithm will (if some tolerance is given) terminate after finitely many iterations [34]. More specifically, it either provides a CLF or ends up with an empty set of possible remaining values of parameters (up to a given tolerance).

3 Generic Algorithm

In this section, we give a brief generic version of the algorithm. Later, we will narrow this generic version to a concrete algorithm using control laws based on linearization around precomputed trajectories, and study the properties of the resulting algorithm.

The algorithm will be based on a demonstrator that, for any given initial point x_0 , generates control

input that steers system (1) from x_0 to the ϵ_0 -neighborhood H^{ϵ_0} of the equilibrium without leaving a set $S \supset D$ that is fixed for the given demonstrator. We will also assume for that all those demonstrations have some fixed finite length T . Although, some demonstrations visits ϵ_0 -neighbourhood sooner than others in practice and hence can be shortened in the implementation to reduce a number of states in a database of all computed demonstrations.

Definition 1. A continuous demonstration of length T is a trajectory (x, u) with $x: [0, T] \rightarrow \mathbb{R}^n$ and $u: [0, T] \rightarrow \mathbb{R}^m$ that satisfies the ODE (1), and for which for all $t \in [0, T]$, $(x(t), u(t)) \in S$, and $x(T) \in H^{\epsilon_0}$.

The algorithm is illustrated schematically in Figure 2, and in more details as Algorithm 1, below. In its first phase, demonstrations are used to learn a CLF for the system (1) (see the left loop in Figure 2 which corresponds to Figure 1). This CLF behaves like a Lyapunov function along the given demonstrations in the following sense.

Definition 2. A function L is compatible with a continuous trajectory (x, u) of length T iff for all $t \in [0, T]$,

1. $L(x(t)) > 0$, and
2. $\nabla L(x(t))^T F(x(t), u(t)) < 0$.

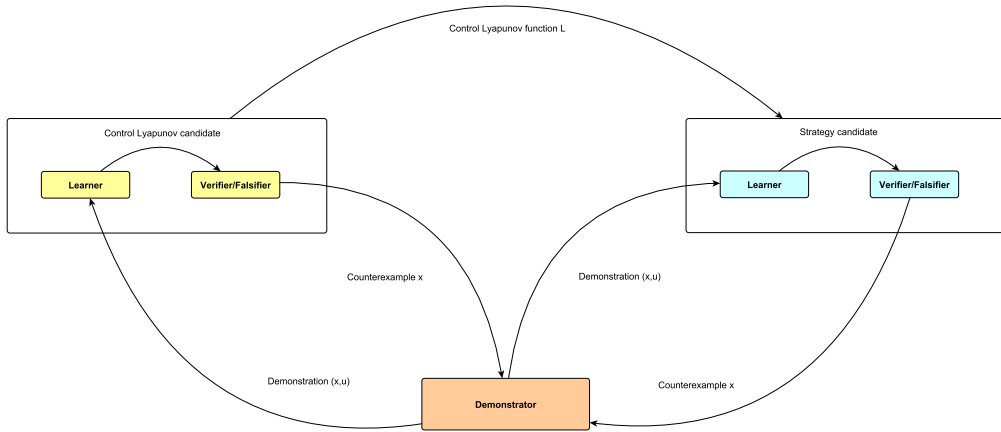


Figure 2: Overview of the algorithm.

Next, such demonstrations are used to define a feedback control law. Then the CLF is used to check if this control law stabilizes the system (this corresponds to the right loop in Figure 2). If a counterexample is found, a new trajectory is generated from the point where the problem was detected and the left loop starts anew. This procedure repeats until no new counterexamples are found. In this case, the procedure as a whole is successful and the CLF confirms stability of the obtained control law. Moreover, since the control law is based on the precomputed trajectories, we can ensure asymptotic optimality relative to the provided demonstrations.

Algorithm 1 Generic Controller Synthesis

Input: A control system $\dot{x} = F(x, u)$

Output: A control law that asymptotically stabilizes the given control system on D

1. Generate an initial set of demonstrations \mathcal{T}
 2. While a stabilizing control law is not found
 - (a) Learn a CLF L using the demonstrations in \mathcal{T} while adding the found counterexamples into \mathcal{T} .
 - (b) Construct a feedback control law u using the current set of demonstrations \mathcal{T} .
 - (c) Test whether the control law u is stabilizing using the CLF L . If a counterexample x is found, generate a demonstration starting from x and add it into \mathcal{T} .
-

Earlier work [36, 34] followed this generic algorithm only partially. In one case [36], only the right loop (learning a control law) is present, while the left loop is omitted. Instead, full system simulations are used to check system stability. In the other case [34], the left loop (learning a CLF) is used and it is the right loop that is skipped and replaced by Sontag’s universal formula.

4 Algorithm with LQR Tracking Control

In this section, we adapt the generic algorithm to a concrete instantiation based on LQR tracking. Namely, the control law will be constructed using time-varying LQR models along the generated demonstrations. Moreover, we formulate stability conditions to check the generated control law and to identify counterexamples. These counterexamples are used as initial points for new demonstrations. The whole checking procedure is based on sampling and we prove asymptotic properties of the algorithm as the number of iterations tends to infinity. This approach of sampling is inspired by motion planning algorithms [36, 43] in which the trajectories also provide a basis for the construction of a global stabilizing control law.

A key part of the algorithm is the set of trajectories provided by the demonstrator. We assume that the demonstrator somehow takes into account the cost functional (2), although the result does not necessarily have to be optimal.

The path to the resulting algorithms will be as follows. First, in Section 4.1, we revisit the construction of LQR tracking control laws that provides a basis for the definition of the resulting controller. Then, in Section 4.2, we prove a stability condition that we use for proving the stability of the system with the controller. And finally, in Section 4.3, we provide the algorithm and prove its asymptotic properties.

4.1 Control Laws from Demonstrations using LQR Tracking

It would be possible to view the demonstrator itself as a feedback control law that periodically computes a demonstration from the current point and uses the corresponding control input for a certain time period. However, this has two disadvantages: First, the run-time of the demonstrator might be too long for real-time usage. Second, the control law provided by the demonstrator is defined implicitly using numerical optimization, which makes further analysis of the behavior (e.g., formal verification) of the resulting closed loop system difficult. To define a control law that both allows for an efficient implementation, and is easier to analyze, we will use linearization along demonstrations, and more specifically, LQR tracking, for which we refer to reader to the literature [22, 19, 43, 36]. Here, we just emphasize the assumption that the quadratic cost used for LQR tracking is positive definite to ensure that the optimal control problem is well posed.

For further reference, we establish the following notation. We denote the controller that asymptotically stabilizes the system around the ϵ_0 -neighborhood H^{ϵ_0} of the equilibrium by $u_{\text{LQR}}^{\text{eq}}$. We denote the LQR trajectory tracking control law, a function in $\mathbb{R}^n \times [0, \infty] \rightarrow \mathbb{R}^m$, by $u_{\text{LQR}}^{(\tilde{x}, \tilde{u})}$, where (\tilde{x}, \tilde{u}) denotes the followed trajectory, which we will call *target trajectory*.

We will now investigate some properties of LQR tracking control. Here we assume that the demonstrator computes, for a given state $x_0 \in D$, a continuous demonstration (x, u) with $x(0) = x_0$. We assume that for every t , the input u at time t is continuous as a function of the initial state x_0 . This assumption will be necessary for the convergence guarantees of our algorithms, although the algorithms can also be used without it. The following proposition, whose proof the reader can find in the appendix, extends the assumed continuity of the demonstrator to LQR tracking trajectories.

Proposition 1. *Every LQR tracking trajectory $\Sigma(x_0, u_{\text{LQR}}^{(\tilde{x}, \tilde{u})}) : [0, T] \rightarrow \mathbb{R}^n$ is, as a function of time, its initial state x_0 and the initial state $\tilde{x}(0)$ of its target trajectory \tilde{x} uniformly continuous on $[0, T] \times D \times D$.*

The continuity of LQR tracking trajectories allows us to investigate their cost in comparison to the cost of the demonstrator. We mentioned earlier that we construct the controller based on demonstrations to reflect the chosen cost. Since demonstrations have finite length, we adapt the cost functional V to the finite horizon case, by defining for a trajectory (x, u) with $x : [0, T] \rightarrow \mathbb{R}^n$ and $u : [0, T] \rightarrow \mathbb{R}^m$, and for $t \in [0, T]$,

$$V_t(x, u) := \int_0^t Q(x(\tau)) + R(u(\tau)) d\tau. \quad (3)$$

This cost of any LQR tracking trajectory converges to the cost of the followed trajectory as their initial points converge (see the appendix for a proof).

Proposition 2. *Let (\tilde{x}, \tilde{u}) be a continuous trajectory of length T . Then for all $t \in [0, T]$,*

$$\left| \text{cost}_{V_t}(x_0, u_{\text{LQR}}^{\tilde{x}, \tilde{u}}) - \text{cost}_{V_t}(\tilde{x}(0), \tilde{u}) \right| \rightarrow 0$$

as $x_0 \rightarrow \tilde{x}(0)$.

Hence, if we choose a suitable demonstrator (in terms of its cost) and sample the state space with demonstrations thoroughly enough, we obtain the control law that will closely mimic the performance of the demonstrator. However, we can generate only finitely many demonstrations in practical terms. And thus, we need to determine when the set of demonstrations is sufficient to our needs. The minimum requirement on the set of demonstrations is stability of the system with LQR tracking based on these demonstrations. And this is the requirement that we will use for our algorithm.

4.2 LQR Switching Control

Assume that we have found a CLF L on the investigated set D that is compatible with the same set of demonstrations \mathcal{T} that we use for the construction of LQR tracking. Our goal is to construct a continuous time feedback control law that exploits

- the presence of a whole *set* of demonstrations instead of a single one, and
- the knowledge of the CLF L .

Hence, instead of just following a single demonstration [36], we will follow a given target trajectory only for some time period t_{switch} , then re-evaluate whether the current target trajectory is still the most convenient one, and switch to a different one, if it is not. Based on this, we will determine stability by relating the point $x(0)$ and the terminal point $x(t_{\text{switch}})$ to the CLF L .

When switching trajectories, the question is, which new target trajectory to choose. One natural possibility is based on the standard Euclidean distance between the current point and the initial point of trajectories in \mathcal{T} . However this metric does not take the dynamics of the system and the cost into account. Another (computationally more expensive) possibility is to use the solution of the Riccati equation used for LQR tracking, since it represents the approximated cost of the tracking [8].

We will assume for the following considerations, that some predefined rule ϕ of the following form was chosen.

Definition 3. *An assignment rule ϕ is a function that for any set of demonstrations \mathcal{T} and point $x \in D$ selects an element from \mathcal{T} . We will say that such an assignment rule is dominated by the Euclidean norm iff for every $\alpha > 0$ there is a $\beta > 0$ such that for every set of demonstrations \mathcal{T} , for every $(\tilde{x}, \tilde{u}) \in \mathcal{T}$ and $x_0 \in D$ with $\|x_0 - \tilde{x}(0)\| < \beta$, there exists a $(\tilde{x}', \tilde{u}') \in \mathcal{T}$ s.t. $\phi(\mathcal{T}, x) = (\tilde{x}', \tilde{u}')$, and $\|x_0 - \tilde{x}'(0)\| < \alpha$, where $\|\cdot\|$ denotes the Euclidean norm.*

Now we can define a control law that switches the target trajectory to the one selected by an assignment rule in certain time intervals.

Definition 4. *Assume a set of demonstrations \mathcal{T} of length T , and an assignment rule ϕ , and let $t_{\min} > 0$. An LQR switching control law based on \mathcal{T} , ϕ , and t_{\min} is a function $u_{\text{switch}}^{\mathcal{T}}: \mathbb{R}^n \times [t_0, \infty) \rightarrow \mathbb{R}^m$ such that for every $x_0 \in \mathbb{R}^n$ there are t_1, t_2, \dots (that we call switching times) and corresponding target trajectories $(\tilde{x}_1, \tilde{u}_1), (\tilde{x}_2, \tilde{u}_2), \dots \in \mathcal{T}$ such that for every $j \geq 0$, $t_{\min} \leq t_{j+1} - t_j \leq T$, and for $t = 0$, as well as for all $t \in (t_j, t_{j+1}]$,*

$$u_{\text{switch}}^{\mathcal{T}}(x, t) = u_{\text{LQR}}^{\phi(\mathcal{T}, \Sigma(x_0, u_{\text{switch}}^{\mathcal{T}})(t_j))}(x, t - t_j),$$

with $t_0 = 0$.

Note that this definition is not circular, since $u_{\text{switch}}^{\mathcal{T}}(x, t)$ on the left-hand side only depends on $u_{\text{switch}}^{\mathcal{T}}(x, t')$ with $t' < t$ on the right-hand side of the equation. Also note that for a fixed initial point x_0 , $u_{\text{switch}}^{\mathcal{T}}(x_0, t)$ is piecewise continuous in t . And finally, observe that unlike LQR tracking, such an LQR switching control law is *not* unique due to the non-unique switching times.

Such a switching control law has the same asymptotic cost properties as pure LQR tracking (see the appendix for a proof).

Proposition 3. Let (\tilde{x}, \tilde{u}) be a continuous trajectory of length T . For every LQR switching control law $u_{\text{switch}}^{\mathcal{T}}$ based on a set of demonstrations \mathcal{T} , an assignment rule ϕ dominated by the Euclidean metric, and $t_{\min} > 0$, for all $t \in [0, T]$,

$$|\text{cost}_{V_t}(x_0, u_{\text{switch}}^{\mathcal{T}}) - \text{cost}_{V_t}(\tilde{x}(0), \tilde{u})| \rightarrow 0$$

as $x_0 \rightarrow \tilde{x}(0)$.

Now we want to use the CLF L to ensure stability of the resulting control law. For this, we will use a stability criterion similar to finite-time Lyapunov functions [2]. We chose constants $1 > \gamma > 0$, $t_{\min} > 0$ and define LQR switching control with Lyapunov function L in such a way that we switch trajectories after the minimum time t_{\min} elapsed, the system is in \mathring{D} , and the following decrease condition is met.

Definition 5. An LQR switching control law $u_{\text{switch}}^{\mathcal{T}}$ is sufficiently decreasing wrt. a function $L : D \rightarrow \mathbb{R}$ iff for every x_0 with corresponding switching times t_1, t_2, \dots and corresponding target trajectories $(\tilde{x}_1, \tilde{u}_1), (\tilde{x}_2, \tilde{u}_2), \dots$ of $u_{\text{switch}}^{\mathcal{T}}$, for $x = \Sigma(x_0, u_{\text{switch}}^{\mathcal{T}})$, for every $j \geq 0$, $x(t_{j+1}) \in \mathring{D}$, and

$$L(x(t_{j+1})) - L(x(t_j)) \leq \gamma [L(\tilde{x}_j(t_{j+1} - t_j)) - L(\tilde{x}_j(0))],$$

and for all $t \in [t_j, t_{j+1}]$, $(x(t), u(t)) \in S$. Here $t_0 = 0$.

Since such a control law decreases L at least by

$$\sup_{(\tilde{x}, \tilde{u}) \in \mathcal{T}} \gamma [L(\tilde{x}(t_{\min})) - L(\tilde{x}(0))]$$

over one trajectory switch, the system must visit H^{ϵ_0} after finitely many trajectory switches. This is formalized by the following proposition whose proof the reader will find in the appendix.

Proposition 4. Let $L : D \rightarrow \mathbb{R}$ be continuously differentiable, positive on $D \setminus H^{\epsilon_0}$ and compatible with a set of demonstrations \mathcal{T} . Then any system trajectory wrt. an LQR switching control law that is sufficiently decreasing wrt. L stays in S , and visits H^{ϵ_0} after finitely many trajectory switches.

Since we assumed that the system (1) has an asymptotically stabilizing controller that we can use around the equilibrium, we can simply switch to this controller around the equilibrium to gain a controller that is asymptotically stabilizing on D .

Corollary 1. Let $L : D \rightarrow \mathbb{R}$ be continuously differentiable, positive on $D \setminus H^{\epsilon_0}$ and compatible with a set of demonstrations \mathcal{T} . Then the system (1) with an LQR switching control law that is sufficiently decreasing wrt. L , and switches to $u_{\text{LQR,eq}}$ when the system visit H^{ϵ_0} , stays in S and is asymptotically stable on D .

4.3 Controller Synthesis Algorithms and their Properties

It is time to instantiate the general algorithm from Section 3 to the LQR switching control law from Definition 4 using Proposition 4. First, in Subsection 4.3.1, we present a simplified version of our algorithm that assumes that a CLF L compatible with this demonstrator is known beforehand. We introduce this simplified algorithm first, to make it easier for the reader to understand the full algorithm that does not depend on a known CLF, and that we introduce in Subsection 4.3.2.

4.3.1 Controller Synthesis with Known Compatible CLF

Let us start with the case in which a suitable CLF compatible with the demonstrator is known beforehand. The result is Algorithm 2 which represents the right loop of the generic algorithm in Figure 2. The left loop (CLF learning) disappeared since a suitable CLF is already provided. The algorithm concretizes the construction of a generic control law to a test whether the constructed LQR switching control law is sufficiently decreasing which, due to Corollary 1, ensures stability.

The loop in the algorithm does not state any termination condition. We will return to this issue later. For now, we will informally discuss why the algorithm produces a stabilizing control law after finitely many iterations—we will formalize the statement in 5 whose proof the reader will find in the appendix.

We first observe that every demonstration reaches a point in H^{ϵ_0} , and hence a point in the interior of D . Moreover, the algorithm requires that the given CLF L is compatible with the trajectories that the demonstrator generates for initial points in $D \setminus H^{\epsilon_0}$. So, for every $x_0 \in D \setminus H^{\epsilon_0}$, and demonstration (x, u) of length T generated by the demonstrator for $x(0) = x_0$, for all $t \in [0, T]$,

$$\nabla L(x(t))^T F(x(t), u(t)) < 0. \quad (4)$$

Algorithm 2 Controller Synthesis with Known Compatible CLF

Input:

- a control system of the form stated in Section 2
- a compact set $D \subseteq \mathbb{R}^n$
- a bounded open set S
- a demonstrator generating demonstrations of minimal length $t_{\min} > 0$
- a CLF L compatible with the trajectories that the demonstrator generates for initial points in $D \setminus H^{\epsilon_0}$

Parameters:

- an assignment rule ϕ dominated by the Euclidean metric
- $1 > \gamma > 0$

Output: A control law that asymptotically stabilizes the given control system on D and optionally satisfies some additional performance requirements

1. Generate an initial set of demonstrations \mathcal{T} .

2. Choose a sequence N of states in $D \setminus H^{\epsilon_0}$ that is dense in $D \setminus H^{\epsilon_0}$, and let $i = 1$.

3. Loop

(A) Let x_0 be the i -th sample N_i , and $x = \Sigma(x_0, u_{\text{LQR}}^{\tilde{x}, \tilde{u}})$, and $(\tilde{x}, \tilde{u}) = \phi(\mathcal{T}, x_0)$, let T be the length of \tilde{x} , and check if there is a $t \in [t_{\min}, T]$ s.t. $x(t) \in \overset{\circ}{D}$, s.t. for all $\tau \in [t_{\min}, t]$, $x(\tau) \in S$, and s.t.

$$L(x(t)) - L(x(0)) < \gamma [L(\tilde{x}(t)) - L(\tilde{x}(0))].$$

If this condition does not hold, generate a new demonstration starting from x_0 and add it to \mathcal{T} .

(B) $i \rightarrow i + 1$

4. return an LQR switching control law based on \mathcal{T}

If we choose our assignment rule ϕ to be dominated by the Euclidean norm, necessarily $\phi(x_0, \mathcal{T}) = (x, u)$, thus $\Sigma(x_0, u_{\text{LQR}}^{\phi(\mathcal{T}, x_0)}) = x$, and therefore for any $t \in [t_{\min}, T]$

$$L\left(\Sigma(x_0, u_{\text{LQR}}^{\phi(\mathcal{T}, x_0)})(t)\right) - L\left(\Sigma(x_0, u_{\text{LQR}}^{\phi(\mathcal{T}, x_0)})(0)\right) < \gamma [L(x(t)) - L(x(0))]. \quad (5)$$

Consequently, any initial point of any demonstration meets the condition checked in the algorithm. Thus if any counterexample x_c is found, adding the demonstration starting from x_c will remove it. Furthermore, due to the uniform continuity of LQR tracking as seen in Proposition 1, and due to the fact that ϕ is dominated by the Euclidean metric, all counterexamples in some neighbourhood of x_c will be eliminated, as well.

Hence, if no further counterexamples exists, we can construct a control law as described in Definition 4 and switch trajectories, when the conditions of Definition 5 are met. Thanks to Corollary 1, such a controller will reach the ϵ_0 -neighbourhood H^{ϵ_0} of the equilibrium, where we assumed that a stabilizing controller exist. Putting everything together, the algorithm constructs (via finding a suitable system of demonstrations) a stabilizing control law. Moreover, the Algorithm 2 does so in finitely many iterations, i.e. only finite number of trajectories are needed (see the appendix for the proof).

Proposition 5. *Algorithm 2 provides a stabilizing control law in finitely many iterations.*

The remaining question is, how to detect that the number of loop iterations is already large enough. In industry, safety-critical systems are often verified by systematic testing. This can be reflected in the termination condition for the main loop by simply considering each loop iteration that does not produce a counter-example as a successful test. Based on this, one could terminate the loop after the number of loop iterations that produced a successful test without any intermediate reappearance of a counterexample exceeds a certain threshold. One could also require certain coverage of the set D with successful tests. And for even stricter safety criteria, one can do formal verification of the resulting controller.

The user might also have additional performance requirements. For ensuring those, we can use the following corollary of Proposition 3.

Corollary 2. *Let x_0^1, x_0^2, \dots be a sequence of states in $D \setminus H^{\epsilon_0}$ that is dense in $D \setminus H^{\epsilon_0}$. Let $(\tilde{x}_1, \tilde{u}_1), (\tilde{x}_2, \tilde{u}_2), \dots$ be the sequence of corresponding demonstrations generated by the demonstrator for $\tilde{x}_1(0) = x_0^1, \tilde{x}_2(0) = x_0^2, \dots$. For $k = 1, \dots$, let $\mathcal{T}_k = \{(\tilde{x}_i, \tilde{u}_i) \mid i \in \{1, \dots, k\}\}$, and $u_{\text{switch}}^{\mathcal{T}_k}$ a corresponding LQR switching control law. Then*

$$\lim_{k \rightarrow \infty} \left| \text{cost}_{V_i}(x_0, u_{\text{switch}}^{\mathcal{T}_k}) - \text{cost}_{V_i}(x_0, u) \right| \rightarrow 0$$

In particular, the limit converges to an optimal controller, if the demonstrator provides optimal demonstrations. Consequently, if we sample the state space thoroughly enough, the cost of the control law will approach the cost of the demonstrator, and hence we can ensure the additional performance requirements by stating the termination condition of the algorithm via performance comparison with the demonstrator. To ensure dense sampling, the algorithm must continue to add demonstrations even in cases where the test for the condition $L(x(t)) - L(x(0)) < \gamma [L(\tilde{x}(t)) - L(\tilde{x}(0))]$ already succeeds.

4.3.2 Controller Synthesis without Known Compatible CLF

In the previous section, we assumed that a CLF compatible with the demonstrator was known. Now, we generalize the algorithm for the case in which a compatible CLF is not known and thus a suitable CLF candidate needs to be learned. The result is Algorithm 3 which now corresponds to the full generic algorithm, as illustrated in Figure 2. In a similar way as in related work [34], the algorithm works with a system of linearly parametrized CLF candidates $L_p(x)$ and finds parameter values p such that the resulting function L_p satisfies the necessary conditions. The set of candidates $\{L_p(x) \mid p \in P\}$ needs to be large enough to contain a CLF compatible with the demonstrations that the demonstrator generates, otherwise, the algorithm may fail.

The main difference to the algorithm from the previous section is the added line (A) and the new loop (a)–(b), which corresponds to the approach for learning control Lyapunov functions [34] that we already described in more detail in the section on related work. This part also represents the left loop of the general layout in Figure 2, i.e. a CLF learner and a chosen CLF verifier (or falsifier). The learner computes a CLF candidate by choosing one which is compatible with all demonstrations and the verifier (falsifier) checks that the given candidate is positive definite. If there is no such candidate, the algorithm fails. The positive definite candidate then serves the same role as a CLF in the first algorithm for falsification of the constructed control law.

Algorithm 3 Controller Synthesis without Known Compatible CLF

Input:

- a control system of the form stated in Section 2
- a compact set $D \subseteq \mathbb{R}^n$
- a demonstrator generating demonstrations of minimal length $t_{\min} > 0$
- a system of linearly parametrized CLF candidates $L_p(x), p \in P$

Parameters:

- an assignment rule ϕ dominated by the Euclidean metric
- $1 > \gamma > 0$, and

Output: A control law that asymptotically stabilizes the given control system on D and optionally satisfies some additional performance requirements

1. Generate an initial set of trajectories \mathcal{T} .
2. Choose a sequence N of states in $D \setminus H^{\epsilon_0}$ that is dense in $D \setminus H^{\epsilon_0}$ and let $i = 1$.
3. Loop
 - (A) While the CLF candidate L_p is not positive on $D \setminus H^{\epsilon_0}$
 - (a) Learn a CLF candidate L_p on D using trajectories \mathcal{T} by finding parameter values p such that for every demonstration $(x, u) \in \mathcal{T}$,
 - (i) $L_p(x) > 0$, and
 - (ii) $\nabla L_p(x)^T F(x, u) < 0$.
 - (b) Find counterexamples to the condition

$$L_p(x) \text{ is positive on } D \setminus H^{\epsilon_0}$$

and add respective trajectories into \mathcal{T}

- (B) Let x_0 be the i -th sample N_i , where $x = \Sigma(x_0, u_{\text{LQR}}^{\tilde{x}, \tilde{u}})$, and $(\tilde{x}, \tilde{u}) = \phi(\mathcal{T}, x_0)$, let T be the length of \tilde{x} , and check if there is a $t \in [t_{\min}, T]$ s.t. $x(t) \in \overset{\circ}{D}$, s.t. for all $\tau \in [t_{\min}, t]$, $x(\tau) \in S$, and s.t.

$$L_p(x(t)) - L_p(x(0)) < \gamma [L_p(\tilde{x}(t)) - L_p(\tilde{x}(0))].$$

If this condition does not hold, generate a new demonstration starting from x_0 and add it to \mathcal{T} .

- (C) $i \rightarrow i + 1$

4. return an LQR switching control law resulting from \mathcal{T}
-

In the proof of the variant of Proposition 5 for Algorithm 3, we need to address the fact, that a CLF candidate can change during the run of algorithm. However, a key observation is that the number of these changes is inherently finite. Let \mathcal{T} be a set of trajectories provided by the demonstrator starting from various initial points and let $\{L_p(x) \mid p \in P\}$ be a linearly parametrized system of continuously differentiable functions. First, we learn a candidate $L_p(x)$ from the linearly parametrized system of function $\{L_p(x) \mid p \in P\}$ that is compatible with all demonstrations in \mathcal{T} .

Proposition 4 also requires the function L to be positive on $D \setminus H^{\epsilon_0}$, and this is the next condition the algorithm checks. If there exists any counterexamples to this condition, we add corresponding trajectories starting from these into \mathcal{T} (though it should be noted that only adding conditions $L_p(x) > 0$ without generating any demonstrations suffices to make the algorithm work). As we already mentioned in the description of related work, these conditions translate to a system of linear inequalities for parameters p and all solutions will lie in some polyhedron contained in P . Moreover, if we choose a candidate $L_p(x)$ as a centre of maximum volume ellipsoid, the volume of the set of admissible parameters decreases at least by a factor [34, 42]

$$V_{\text{new}} \leq \left(1 - \frac{1}{d}\right) V_{\text{old}},$$

where d is number of parameters. Let us assume some terminal condition on the minimum volume of the admissible set of parameters. If we reach this condition, we terminate the learning algorithm. Hence, we will either find a candidate compatible with \mathcal{T} or fail in finitely many iterations.

Consequently, we can assume that we have a candidate $L_p(x)$ compatible with \mathcal{T} , but that does not mean that the candidate is compatible with \mathcal{T}_{all} , the set of all possible demonstrations. Nevertheless, as our algorithm progresses, more and more trajectories are added and it can happen, that an added trajectory is not compatible with the current candidate $L_p(x)$. Thus, we have to update our candidate by adding more constraints but again regardless of which new counterexample constraint is added, the admissible set of parameters decreases at least by the factor $(1 - \frac{1}{d})$. Hence, we can add at most finitely many counterexample constraints until we learn a candidate $L_p(x)$ compatible with all trajectories generated during the run of the algorithm or fail. In other words, our candidate $L_p(x)$ can change during the run of the whole algorithm at most finitely many times. This observation allows us to state the following proposition (see the appendix for a detailed proof).

Proposition 6. *Algorithm 3 either fails or provides a stabilizing control law in finitely many iterations.*

In the same way as for Algorithm 2, we can again use Corollary 2 to continue to add demonstrations even if the tests already succeed, in order to satisfy additional performance requirements.

Finally, notice that after enough iterations of the algorithm for any state x_0 from the sequence N of states in $D \setminus H^{\epsilon_0}$ that is dense in $D \setminus H^{\epsilon_0}$, $\nabla L_p(x(t))^T F(x(t), u(t)) < 0$ holds for all t , where (x, u) is the demonstration starting from x_0 . Since N is dense in $D \setminus H^{\epsilon_0}$, and demonstrations are assumed to be continuous with respect to their initial states, and L_p is assumed to be continuous as well, inequality (4) actually holds for any possible demonstration from \mathcal{T}_{all} . Consequently, there is a control (the control provided by the demonstrator itself) that decreases the value of the positive function L_p from any point of $D \setminus H^{\epsilon_0}$, thus L_p is actually a CLF on $D \setminus H^{\epsilon_0}$. Moreover, it is a CLF that is compatible with the chosen demonstrator. It should be noted however that the algorithm can succeed in creating a stabilizing controller *before* L_p becomes a CLF, i.e. having a set of candidates that does not include a CLF compatible with the respective demonstrator does not inherently imply that the algorithm fails in creation of a stabilizing controller.

5 Discrete Demonstrations and Implementation of LQR Algorithm

Up to now, all algorithms have been based on the ideal case of continuous system trajectories. However, computer simulations work with discrete approximations [16]. In Subsection 5.1 we discuss, how to take this into account for the LQR switching control from Section 4.2 and present the consequences for our algorithms. In Subsection 5.2 we discuss further details of the implementation of Algorithm 3 that we used for the computational experiments that we will describe in the next section.

5.1 Discrete Demonstrations and Discrete Time Conditions

Again we will assume a demonstrator, that now computes discrete demonstrations analogous to Definition 1.

Definition 6. *A discrete demonstration of length T is a pair (x, u) , where both x and u are sequences of the form $x: \{1, \dots, T\} \rightarrow \mathbb{R}^n$ and $u: \{1, \dots, T\} \rightarrow \mathbb{R}^m$, and for which for all $t \in \{1, \dots, T\}$, $(x(t), u(t)) \in S$, and $x(T) \in H^{\epsilon_0}$.*

For simplicity's sake, we assume a constant h that models the step length between two subsequent samples. Again, our convergence results will be based on the assumption that for every $t \in \{1, \dots, T\}$, the input u that the demonstrator computes for time t is continuous as a function of the initial state x_0 which, of course, is a mathematical abstraction of a concrete implementation, where floating point computation is a fundamental obstacle to convergence in the precise mathematical sense.

Notice that there is a certain asymmetry with Definition 1 of continuous demonstration. Namely, there is no equivalent to the fact that a continuous demonstration is a solution to ODE (1). A discrete demonstration provided by demonstrator does not need to be a mere *sampled* continuous demonstration. However, to use precomputed discrete controller on continuous system, we need to somehow reconstruct a continuous controller from this discrete demonstration.

Assume a discrete demonstration $(\tilde{x}_d, \tilde{u}_d)$. Since the discussed approach is based on LQR tracking, we choose to reconstruct a continuous demonstration $(\tilde{x}_c, \tilde{u}_c)$ via continuously (piecewise linearly) interpolated discrete LQR tracking [24]

$$u_{\text{LQR}}^{(\tilde{x}_d, \tilde{u}_d)}(x, t) := \tilde{u}_{d,j} - K_j(x - \tilde{x}_j) + \frac{\tilde{u}_{d,j+1} - \tilde{u}_{d,j} - K_{j+1}(x - \tilde{x}_{d,j+1}) + K_j(x - \tilde{x}_{d,j})}{h}(t - h(j-1)), \quad (6)$$

for $t \in \langle h(j-1), hj \rangle$, $j = 1, 2, \dots$, where

$$S_j = Q_{\text{LQR}} + A_j^T(S_{j+1} - S_{j+1}B_j(R_{\text{LQR}} + B_k^T S_{j+1}B_j)^{-1}B_j^T S_{j+1})A_j \quad (7)$$

$$K_j = (R_{\text{LQR}} + B_j^T S_{j+1}B_j)^{-1}B_j^T S_{j+1}A_j \quad (8)$$

($Q_{\text{LQR}}, R_{\text{LQR}}$ are some chosen positive definite matrices) and

$$A_j = I + h \left. \frac{\partial F(x, u)}{\partial x} \right|_{x=\tilde{x}_{d,j}, u=\tilde{u}_{d,j}} \quad (9)$$

$$B_j = h \left. \frac{\partial F(x, u)}{\partial u} \right|_{x=\tilde{x}_{d,j}, u=\tilde{u}_{d,j}}. \quad (10)$$

Hence for any discrete demonstration $(\tilde{x}_d, \tilde{u}_d)$ we have its continuous counterpart $(\tilde{x}_c, \tilde{u}_c)$ with $\tilde{x}_c(t) = \Sigma(\tilde{x}_1, u_{\text{LQR}}^{(\tilde{x}_d, \tilde{u}_d)})(t)$. In addition, the corresponding ODE

$$\dot{x}(t) = F(x(t), u_{\text{LQR}}^{(\tilde{x}_d, \tilde{u}_d)}(x(t), t)) \quad (11)$$

has continuous right hand side in all arguments and is locally Lipschitz in x , uniformly in t and $\tilde{x}_d(0)$. That holds due to our assumptions, since F is assumed to be smooth and $u_{\text{LQR}}^{(\tilde{x}_d, \tilde{u}_d)}$ is continuous as a function of time and initial state $\tilde{x}_d(0)$. Hence, the LQR tracking trajectory $\Sigma(x_0, u_{\text{LQR}}^{(\tilde{x}_d, \tilde{u}_d)}): [0, T] \rightarrow \mathbb{R}^n$ is, as a function of time, its initial state x_0 and the initial state of its target trajectory $\tilde{x}_d(0)$ uniformly continuous on $[0, T] \times D \times D$.

So, not only the continuous counterpart $(\tilde{x}_c, \tilde{u}_c)$ of the discrete demonstration $(\tilde{x}_d, \tilde{u}_d)$ meets our continuity assumptions with respect to initial states, but also this new interpolated one LQR tracking meets Proposition 1 as well. Hence, the discrete case can be converted to the continuous one with discrete demonstrations replaced by their continuous counterparts and LQR tracking replaced by its interpolated discrete time variant. Only one further assumptions must be added to make the conversion fully work. We must ensure that the continuous demonstrations $(\tilde{x}_c, \tilde{u}_c)$ meets our remaining criteria on continuous demonstrations, that is, they stay in S and end in H^{ϵ_0} . In the implementation itself, this can be checked simply via a simulation before the corresponding demonstration is added.

However, it is convenient to keep working in discrete time for the purpose of the implementation. This can be done easily by replacing the original compatibility condition from Definition 2 with its discrete time counterpart that we describe next. Notice that in the case of discrete demonstrations, we will just need to know the original discrete demonstrations, their sampled continuous counterparts (not the whole continuous demonstrations) and the matrices that define discrete LQR tracking and hence, we need only discrete time objects.

Assume a continuous demonstration (\tilde{x}, \tilde{u}) provided directly by a demonstrator or computed using a discrete demonstration using LQR tracking. We define discrete time compatibility with L simply as

Definition 7. A function $L: \mathbb{R}^n \rightarrow \mathbb{R}$ is discretely compatible with a continuous demonstration (\tilde{x}, \tilde{u}) of length T for $h > 0$ iff

1. for all $t \in \{0, h, 2h, \dots, T\}$, $L(\tilde{x}(t)) > 0$, and

2. for all $t \in \{0, h, 2h, \dots, T - h\}$, $L(\tilde{x}(t + h)) - L(\tilde{x}(t)) < 0$.

We also easily adapt the LQR switching control (Definition 4) for the discrete time compatibility case by requiring that the switching times are multiples of h . If our original demonstrations are discrete, we also use interpolated discrete LQR tracking instead of the continuous one. The next result immediately follows from Proposition 4.

Corollary 3. *Let $L : D \rightarrow \mathbb{R}$ be continuous, positive on $D \setminus H^{\epsilon_0}$, and discretely compatible with a set of continuous demonstrations \mathcal{T} for some $h > 0$. Then any system trajectory wrt. an LQR switching control law that has switching times that are multiples of h , and that is sufficiently decreasing wrt. L stays in S , and visits H^{ϵ_0} after finitely many trajectory switches.*

According modifications of Algorithms 2 and 3 are also straightforward. The CLF learning conditions are replaced by the discrete ones from Definition 7 and the compatibility condition is again evaluated for time instants that are multiples of h . The analogic propositions corresponding to Propositions 5 and 6 also holds (the proof is analogous to the continuous time conditions which is enclosed in the appendix).

Proposition 7. *Algorithm 2 for discrete time conditions provides a stabilizing control law in finitely many iterations and Algorithm 3 for discrete time conditions either fails or provides a stabilizing control law in finitely many iterations.*

5.2 Implementation of Algorithm 3 for Discrete Demonstrations

We comment on the implementation used for the case studies. The implementation is quiet similar to the original Algorithm 3 with the modifications described in the previous subsection, i.e. demonstrations are discrete and compatibility is checked in the discrete-time sense. The LQR tracking control is based on the linearly interpolated discrete-time LQR control (6), where cost matrices $Q_{\text{LQR}}, R_{\text{LQR}}$ are free parameters that depends on the particular problem.

Concerning the choice of an assignment rule ϕ from Definition 3, we choose a combination of the Euclidean norm and the approximated cost of the LQR tracking gained from (6). Namely, we narrow the search of the target trajectory via the Euclidean distance (we find 100 closest trajectories) and then choose the one with the smallest estimated tracking cost in order to reduce computation time for large sets of trajectories.

We should also mention that LQR switching control law is not defined uniquely due to the choice of the switching times. For our implementation, we always choose as the switching time the first allowed time instant within the interior of D . We also always check this time instant for the purpose of the falsifier. Hence, if the compatibility condition is not met in this time instant, we regard a simulation as a failure regardless of future states where the condition might be met.

Since we realize only a finite version of the algorithm, we will also assume a uniform random sampling of the state space for finding counterexamples to the compatibility condition in Definition 7. It should be noted that if we make sure that every infinite realization sampling is dense (except the realizations of the corresponding probability measure zero), we can easily state the probabilistic versions of Propositions 5 and 6. For the finite realizations of the algorithm, we use the following termination criterion: Finish the loop, accepting the current strategy as stabilizing, if the number of simulations without finding a counterexamples exceeds a certain threshold. If we generate N samples without finding any counterexample, by the rule of three, the estimate of a 95% confidence interval for the probability to generate a sample that fails the condition is $[1 - \frac{1}{N}, 1]$.

Further, we do not generate demonstrations due to the existence of counterexamples with positive definiteness of CLF candidates, since they are not required. All that is need is to add inequality $L(x_c) > 0$ for a counterexample x_c into a current set of inequalities that is used for the generation of CLF candidates. On the subject of demonstrations, every discrete demonstration is interpreted as a set of discrete demonstrations from each point of the discrete demonstration to its end. This implies that with each added demonstration actually multiple trajectories are added into the set of current system of trajectories. Such a modification does have any influence on the inferred theoretical results whatsoever.

The whole implementation wasa done in MATLAB 2018b [46]. We chose our demonstrator as a direct optimal control solver [9] that solves the nonlinear programming problem which is obtained from the optimal control problem by discretization of the system dynamics and the cost [9]. The demonstrator is constructed using the toolbox CasADi [5] with the internal non-linear optimization solver Ipopt [47] (the discretization is done via the Hermite-Simpson collocation method [17]). The Lyapunov candidate learner is implemented in the toolbox YALMIP [26] with the semidefinite programming solver SDPT3 [44]. Positive definiteness of the Lyapunov candidate is checked via a falsifier based on the differential evolution algorithm best/1/bin [31].

Case study	Total (pure sim.)	Last (pure sim.)	Total (Lyap.)	Last (Lyap.)
Pendulum	90	87	42	41
Cart pendulum	802	408	664	196
RTAC	42486	6019	1116	491
Acrobot	10996	8723	6786	3981
Fan	7337	4273	5803	1290

Table 1: Simulations time (total time and time in the last iteration): Comparison of a pure simulation algorithm described in Example 1 and Algorithm 3.

The initial solutions for the demonstrator is set as constant zero as all zero solution for both states and control with the exception of initial states. Otherwise, all solvers us their respective default settings.

6 Examples

In this section, we provide computational experiments documenting the behavior of our algorithm and implementation on five typical benchmark problems. For each problem, we also provide a comparison of the resulting feedback controller with Sontag’s formula, and with an algorithm using simulation based LQR trees [36], that does not use trajectory switches and evaluates samples using full system simulations. However, we omitted the implementation of control funnels and based the trajectory assignment on the assignment rule that was used for our algorithm. Table 1 summarizes the latter comparison for later reference. Throughout, we will call our algorithm and implementation “Lyapunov based approach”.

All computation was done on a PC with Intel Core i7-4820K, 3.7GHz and 16GB of RAM.

6.1 Example 1: Inverted pendulum

Consider the dynamics of the inverted pendulum

$$\ddot{\theta} = \frac{g}{l} \sin \theta - \frac{b\dot{\theta}}{ml^2} + \frac{u}{ml^2}, \quad (12)$$

where $m = 1, l = 0.5, g = 9.81, b = 0.1$, and quadratic cost

$$V_t(x, u) = \int_0^t \theta(\tau)^2 + \dot{\theta}(\tau)^2 + u(\tau)^2 d\tau \quad (13)$$

and let the region of interest D be $[-4, 4] \times [-6, 6]$ where the first interval corresponds to the angle θ , the second one to the angular velocity $\dot{\theta}$. Moreover, we reduce the set S for the angular velocity to $\dot{\theta} \in [-8, 8]$. A controller based merely on linearization around the equilibrium does not satisfy our criteria, since it leaves the set S . Hence, more trajectories are need to construct a suitable controller.

We choose demonstrations that are 10s long with time step 0.05s. The boundary $\dot{\theta} \in [-8, 8]$ was added as an additional constraint.

We learned a LQR switching control law using our algorithm for the minimum switching time of $t_{\min} = 0.5s$, $\gamma = 0.01$ and $\epsilon_0 = 0.05$. The cost matrices $Q_{\text{LQR}}, R_{\text{LQR}}$ used for construction of LQR tracking was chosen the same as for the cost $V_t(x, u)$ itself. Note that sometimes a suitable quadratic candidate was not found on D and thus we choose to use a polynomial of a higher order (4th order was sufficient) and choose parameters bounds as $[-10, 10]$. The control was accepted after 20000 successful subsequent simulations. In the end, we found the candidate

$$L = -0.019\theta + 8.330\theta^2 - 4.689\theta^3 + 7.490\theta^4 + 0.037\dot{\theta} + 4.326\theta\dot{\theta} - 0.000\theta^2\dot{\theta} + 2.605\theta^3\dot{\theta} + 1.888\dot{\theta}^2 + 0.000\theta\dot{\theta}^2 + 4.492\theta^2\dot{\theta}^2 - 0.721\dot{\theta}^3 + 3.539\theta\dot{\theta}^3 + 1.690\dot{\theta}^4$$

using eight trajectories.

We make a cost comparison on $[-\pi, \pi] \times [-5, 5]$ between the control based on Sontag’s formula for a system $\dot{x} = F(x) + G(x)u$ and our controller. Here, Sontag’s formula takes the form [40, 15]

$$u = \begin{cases} -\frac{a + \sqrt{a^2 + x^T Q x b^2}}{b} G(x)^T \nabla L(x) & \text{if } b \neq 0 \\ 0 & \text{otherwise,} \end{cases} \quad (14)$$

# parameters of L	14
# counterexamples (positive definiteness)	8
# counterexamples (decrease condition)	6
# demonstrations	6
# states in all demonstrations	252
# inequalities	82
Demonstrator time	0.84s
Learner time	10.58s
Falsifier (positive definiteness) time	28.69s
Falsifier (decrease condition) time	41.67s
Falsifier (decrease condition) simulations	20127
Total time	88.40s

Table 2: The run of the algorithm for the inverted pendulum example

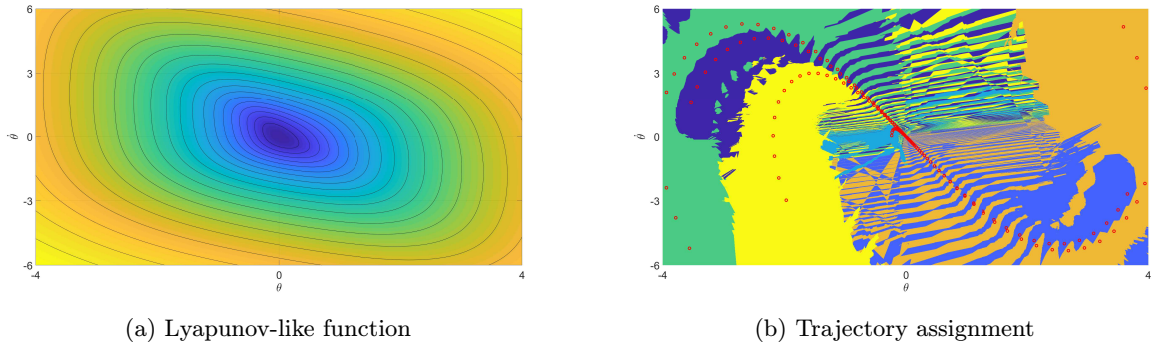


Figure 3: Pendulum: polynomial (4th order) Lyapunov-like function compatible with the learned control for the pendulum (logarithmic scale) and trajectory assignment (colours corresponds to each respective demonstration)

where $a = \nabla L(x)^T F(x)$, $b = \nabla L(x)^T G(x)G(x)^T \nabla L(x)$, and $q : \mathbb{R} \mapsto \mathbb{R}$ such that $q(0) = 0$, and $bq(b) > 0$ for any non-zero b , and $Q = I$ in our example.

We learned a quadratic CLF on $[-10, 10] \times [-10, 10]$ using demonstrations from the same demonstrator as the one we used for our algorithm and checked its properties via falsification through optimization via a differential evolution algorithm that is also used in our algorithm, as described in Subsection 5.2. The resulting CLF was

$$L = 7.50\theta^2 + 3.43\dot{\theta}^2 + 1.74\theta\dot{\theta}.$$

Sontag’s formula provides an optimal control law only if the used CLF and the optimal cost have the same level sets [15]. As can be seen from histogram 5, this is definitely not the case for the Lyapunov function we learned.

In the comparison with the approach based on full simulations we used the same threshold for acceptance of the strategy, that is, 20000 subsequent successful simulations. Three trajectories were added in the simulation-only approach. Moreover, the simulations in the simulation-only approach took 90.3 seconds and 87.0 seconds was needed in the last iteration. The simulations in the Lyapunov approach took 41.7 seconds in total, and the successful iteration took a mere 40.7 seconds with the same number of required simulations. This shows the benefit of learning a Lyapunov-like function to significantly decrease the required simulation time for one whole iteration.

6.2 Example 2: Inverted pendulum on a cart

Assume the model

$$\begin{aligned} \ddot{x} &= \frac{4u + 4ml\dot{\theta}^2 \sin \theta - 3mg \sin \theta \cos \theta}{4(M + m) - 3m \cos^2 \theta} \\ \ddot{\theta} &= \frac{(M + m)g \sin \theta - u \cos \theta - ml\dot{\theta}^2 \sin \theta \cos \theta}{l(\frac{4}{3}(M + m) - m \cos^2 \theta)}, \end{aligned} \tag{15}$$

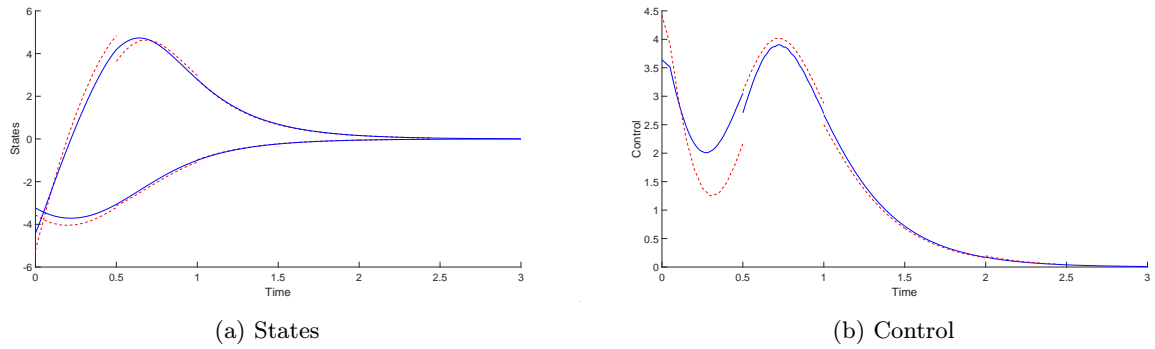


Figure 4: Pendulum: LQR switching control trajectory, red dashed line denotes target trajectories

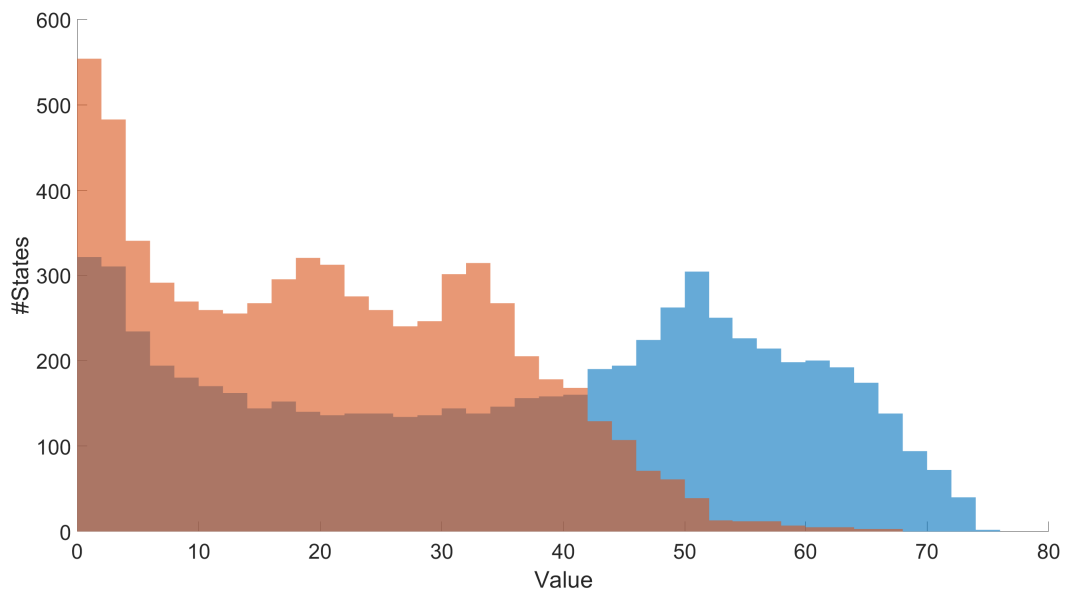


Figure 5: Pendulum: value of Sontag's formula (blue, mean value is 35,2) and the LQR switching control (red, mean value is 20,5)

# parameters of L	10
# counterexamples (positive definiteness)	2
# counterexamples (decrease condition)	29
# demonstrations	29
# states in all demonstrations	3407
# inequalities	235
Demonstrator time	58.5s
Learner time	16.0s
Falsifier (positive definiteness) time	89.1s
Falsifier (decrease condition) time	663.8s
Falsifier (decrease condition) simulations	179800
Total time	494.7s

Table 3: The run of the algorithm for the pendulum on a cart example

that describes an inverted pendulum on a cart. The state x corresponds to the position of the cart and θ is the angle between pendulum and the vertical axis. The goal is to bring the pendulum into vertical position by moving the cart and to keep it there. Hence, we again choose the quadratic cost

$$V_i(y, u) = \int_0^t y(\tau)^T Q y(\tau) + u(\tau)^T R u(\tau) d\tau, \quad (16)$$

for $Q = R = I$, where $y = (x, \theta, \dot{x}, \dot{\theta})^T$.

Let the parameter values of be $m = 0.21$, $M = 0.815$ a $l = 0.305$ and let the region of interest D be $[-2.5, 2.5] \times [-2, 2] \times [-2.5, 2.5] \times [-2.5, 2.5]$ (the order of intervals is $x, \theta, \dot{x}, \dot{\theta}$). We also added a constraint $x \in [-6, 6]$ that both to the demonstrator and the strategy falsifier take into account.

We set demonstrations to be 10s long with a time step 0.05s and set the minimum switching time t_{\min} to 0.5 seconds, $\gamma = 10^{-2}$ and $\epsilon = 0.1$. The LQR tracking cost was chosen also as identity matrices. A quadratic CLF candidate with even powers only (parameters bounded to $P = [-10, 10]^{10}$) was sufficient for this example. The algorithm constructed the candidate

$$L = 0.923x^2 + 3.031x\theta + 9.091\theta^2 + 0.888x\dot{x} + 3.724\theta\dot{x} + 0.808\dot{x}^2 + 0.527x\dot{\theta} + 3.252\theta\dot{\theta} + 0.984\dot{x}\dot{\theta} + 0.525\dot{\theta}^2$$

after adding 29 trajectories when it reached the required 50000 simulations without finding a counterexample.

To make a comparison with Sontag's formula (14), we also learned the CLF using demonstrations checked its properties via falsification as in the previous example

$$L = 0.54x^2 + 1.46x\theta + 9.09\theta^2 + 0.49x\dot{x} + 3.72\theta\dot{x} + 0.90\dot{x}^2 + 0.40x\dot{\theta} + 3.58\theta\dot{\theta} + 1.35\dot{x}\dot{\theta} + 0.85\dot{\theta}^2$$

on $[-2.5, 2.5] \times [-2, 2] \times [-10, 10] \times [-10, 10]$ and used it to compare the cost of the respective control laws on $[-1, 1]^4$, see the histogram in Figure 8.

The simulation-only approach needed fifteen trajectories and simulations took 802 seconds. However, 408 seconds were needed in the last iteration (the control was accepted after 50000 successful simulations). The simulations in the Lyapunov approach took 664 seconds, while the successful iteration took a mere 196 seconds with the same number of required simulations. This again shows a benefit of learning the Lyapunov-like function to significantly decrease the required simulation time.

6.3 Example 3: RTAC (Rotational/translational actuator)

Assume the control-affine model [11]

$$\dot{x} = F(x) + G(x)u, \quad (17)$$

for

$$F = \begin{pmatrix} x_2 \\ \frac{-x_1 + 0.2x_4^2 \sin x_3}{1 - 0.04 \cos^2 x_3} \\ x_4 \\ 0.2 \cos x_3 \frac{x_1 - 0.2x_4^2 \sin x_3}{1 - 0.04 \cos^2 x_3} \end{pmatrix}, \quad G = \begin{pmatrix} 0 \\ \frac{-0.2 \cos x_3}{1 - 0.04 \cos^2 x_3} \\ 0 \\ 0.2 \cos x_3 \frac{1}{1 - 0.04 \cos^2 x_3} \end{pmatrix}. \quad (18)$$

What makes this example interesting is the fact that stabilization of the system is quite long (approximately 50 seconds). This makes full simulations to check stability largely ineffective.

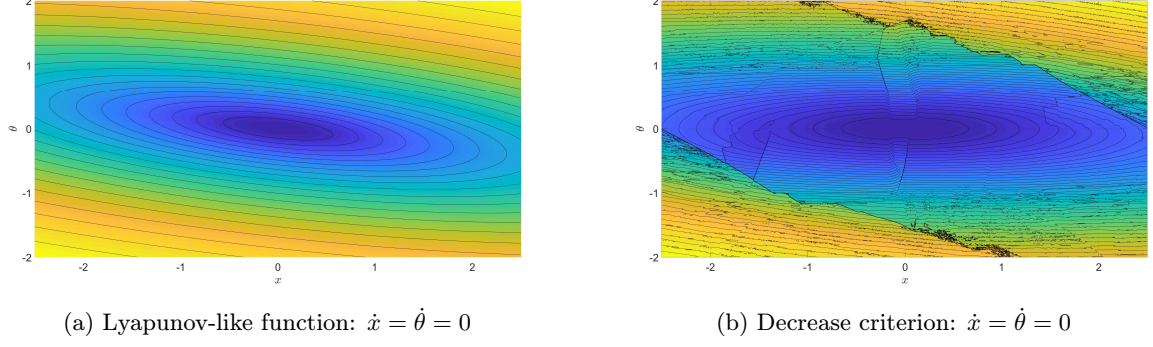


Figure 6: Pendulum on a cart: polynomial (4th order) Lyapunov-like function compatible with the learned control for the pendulum on a cart

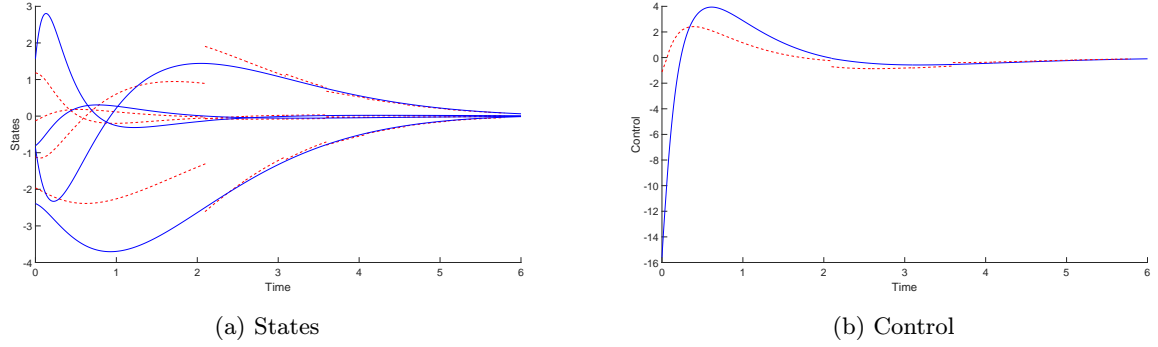


Figure 7: Pendulum on a cart: LQR switching control trajectory, red dashed line denotes target trajectories

For the purpose of this example, we choose the region of interest D as $[-5, 5]^4$. Demonstrations were 150s long with a time step of 0.05s. We set the minimum switching time t_{\min} to 4 seconds, $\gamma = 10^{-2}$, and $\epsilon = 0.05$. The LQR tracking cost $Q_{\text{LQR}}, R_{\text{LQR}}$ are identity matrices. A polynomial CLF of fourth order candidates with even powers only (45 parameters bounded to $P = [-10, 10]^{45}$) was sufficient for this case. The algorithm returned the CLF

$$\begin{aligned}
L = & 3.822x_1^4 - 1.229x_1^3x_2 - 2.878x_1^3x_3 - 5.13x_1^3x_4 + 7.145x_1^2x_2^2 + 6.577x_1^2x_2x_3 + 1.782x_1^2x_2x_4 + \\
& + 8.322x_1^2x_3^2 + 4.4x_1^2x_3x_4 + 5.178x_1^2x_4^2 + 8.546x_1^2 - 1.345x_1x_2^3 - 2.646x_1x_2^2x_3 - 2.242x_1x_2^2x_4 + \\
& + 1.956x_1x_2x_3^2 + 0.929x_1x_2x_3x_4 - 0.285x_1x_2x_4^2 + 0.744x_1x_2 - 3.882x_1x_3^3 + 4.123x_1x_3^2x_4 + \\
& + 2.415x_1x_3 + 2.383x_1x_4^3 - 5.434x_1x_4 + 3.662x_1^4 + 5.029x_2^3x_3 + 2.073x_2^3x_4 + 6.457x_2^2x_3^2 + 7.72x_2^2x_3x_4 + \\
& + 4.319x_2^2x_4^2 + 8.45x_2^2 + 0.703x_2x_3^3 - 5.95x_2x_3^2x_4 + 0.724x_2x_3x_4^2 + 6.304x_2x_3 + 3.079x_2x_4^3 + \\
& + 6.08x_2x_4 + 7.118x_3^4 - 2.218x_3^3x_4 + 3.189x_3^2x_4^2 + 4.276x_3^2 - 0.317x_3x_4^3 + 3.835x_3x_4 + 2.554x_4^4 + 4.355x_4^2
\end{aligned}$$

when reaching the required number of 100000 simulations without finding a counterexample. At this point, 23 trajectories have been added.

To make a comparison with Sontag's formula (14), we also learned the CLF using demonstrations, and checked it via falsification as in the previous example. We used the resulting CLF

$$\begin{aligned}
L = & 5.635x_1^4 - 1.623x_1^3x_2 - 2.324x_1^3x_3 - 3.651x_1^3x_4 + 9.745x_1^2x_2^2 + 2.230x_1^2x_2x_3 + 2.396x_1^2x_2x_4 + \\
& + 7.704x_1^2x_3^2 + 0.9607x_1^2x_3x_4 - 0.274x_1^2x_4^2 + 9.745x_1^2 - 0.023x_1x_2^3 + 4.722x_1x_2^2x_3 - 0.848x_1x_2^2x_4 + \\
& + 8.8805x_1x_2x_3^2 + 9.7446x_1x_2x_3x_4 + 2.3132x_1x_2x_4^2 - 1.6718x_1x_2 - 9.7446x_1x_3^3 + 9.7446x_1x_3^2x_4 + 8.7411x_1x_3x_4^2 - \\
& - 1.296x_1x_3 + 4.927x_1x_4^3 - 7.681x_1x_4 + 5.779x_2^4 + 6.761x_2^3x_3 + 4.158x_2^3x_4 + 9.745x_2^2x_3^2 + 8.530x_2^2x_3x_4 + \\
& + 4.539x_2^2x_4^2 + 9.745x_2^2 + 3.338x_2x_3^3 - 9.745x_2x_3^2x_4 + 5.668x_2x_3x_4^2 + 9.089x_2x_3 + 9.745x_2x_4^3 + \\
& + 6.945x_2x_4 + 9.745x_3^4 + 5.141x_3^3x_4 + 9.745x_3^2x_4^2 + 4.597x_3^2 + 9.745x_3x_4^3 + 5.546x_3x_4 + 7.041x_4^4 + 3.982x_4^2
\end{aligned}$$

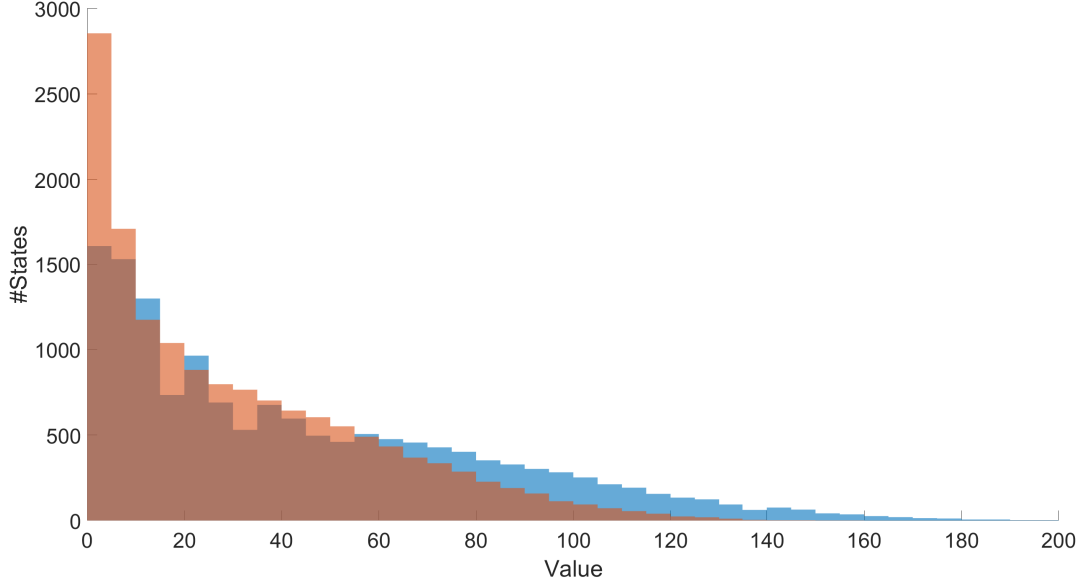


Figure 8: Pendulum on a cart: value of Sontag’s formula (blue, mean value is 44,7) and the LQR switching control (red, mean value is 31,0)

# parameters of L	45
# counterexamples (positive definiteness)	3
# counterexamples (decrease condition)	23
# demonstrations	23
# states in all demonstrations	36428
# inequalities	1667
Demonstrator time	326.2s
Learner time	3478.7s
Falsifier (positive definiteness) time	85.6s
Falsifier (decrease condition) time	1115.5s
Falsifier (decrease condition) simulations	223924
Total time	5316.1s

Table 4: The run of the algorithm for the RTAC example

on $D = [-5, 5]^4$ to compare the cost of the respective control laws on $[-2, 2]^4$, see the histogram in figure 11. Here, computation took 42486 seconds, where 6019 seconds were spent in the last iteration. This in stark contrast to our approach, which took 1116 seconds, and where the successful last iteration took a mere 491 seconds with the same termination criterion. So our approach was twelve times faster, here.

6.4 Example 4: Inverted double pendulum

The inverted double pendulum (or acrobot) is a simple model used for a humanoid robot balancing. The system of ordinary differential equations can be written as [28]

$$M(\theta)\ddot{\theta} + C(\theta, \dot{\theta})\dot{\theta} + G(\theta) = \begin{pmatrix} 0 \\ u \end{pmatrix}, \quad (19)$$

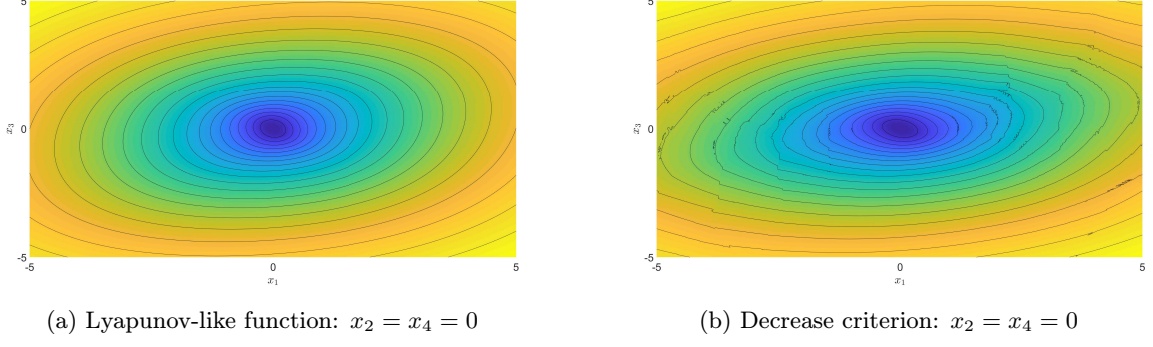


Figure 9: RTAC: polynomial (4th order) Lyapunov-like function compatible with the learned control for the RTAC

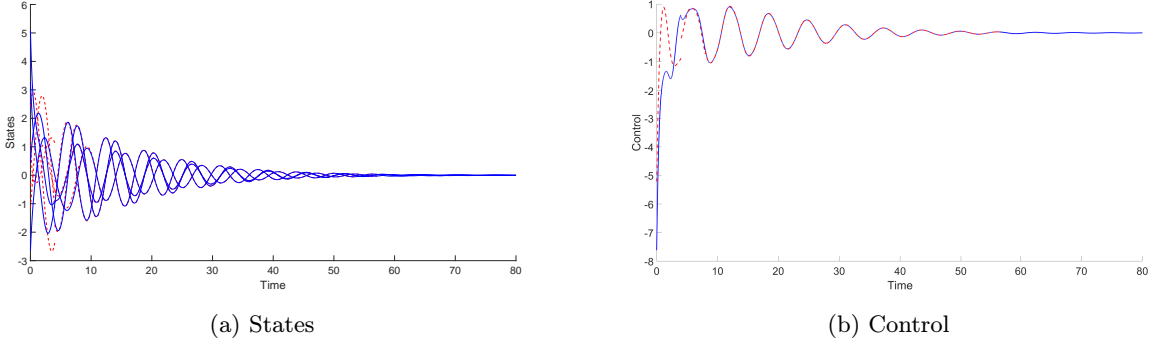


Figure 10: RTAC: LQR switching control trajectory, red dashed line denotes target trajectories

where

$$\begin{aligned}
 M &= \begin{pmatrix} a + b + 2c \cos \theta_2 & b + c \cos \theta_2 \\ b + c \cos \theta_2 & b \end{pmatrix}, \\
 C &= \begin{pmatrix} -c \sin \theta_2 \dot{\theta}_2 & -c \sin \theta_2 (\dot{\theta}_1 + \dot{\theta}_2) \\ c \sin \theta_2 \dot{\theta}_1 & 0 \end{pmatrix}, \\
 G &= - \begin{pmatrix} d \sin \theta_1 + e \sin (\theta_1 + \theta_2) \\ e \sin (\theta_1 + \theta_2) \end{pmatrix},
 \end{aligned}$$

with

$$\begin{aligned}
 a &= m_1 l_1^2 + m_2 l_2^2 & b &= m_2 l_2^2, \\
 c &= m_2 l_1 l_2 & d &= g m_1 l_1 + g m_2 l_2, \\
 e &= g m_2 l_2.
 \end{aligned}$$

The system can be rewritten to the usual control-affine form

$$\ddot{\theta} = \begin{pmatrix} \dot{\theta} \\ -M^{-1}(C\dot{\theta} + G) \end{pmatrix} + \begin{pmatrix} 0 \\ M^{-1} \begin{pmatrix} 0 \\ 1 \end{pmatrix} \end{pmatrix} u. \quad (20)$$

The states of the system are the angles θ_1 and θ_2 and the angular velocities $\dot{\theta}_1$ and $\dot{\theta}_2$. The lengths of pendula are denoted as l_1 and l_2 , their weights as m_1 and m_2 and g denotes the gravitational acceleration. The linearization of the acrobot around its unstable equilibrium $\theta_1 = \theta_2 = \dot{\theta}_1 = \dot{\theta}_2 = 0$ (upward position) is controllable [28].

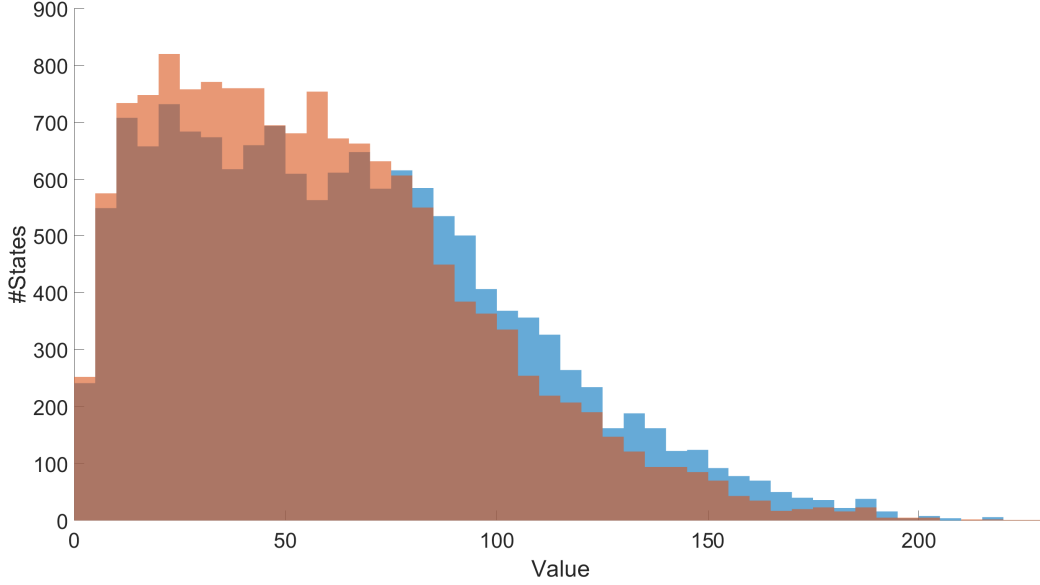


Figure 11: RTAC: value of Sontag's formula (blue, mean value is 64,0) and the LQR switching control (red, mean value is 58,2)

We will use the same values of parameters as in [28], i.e.

$$\begin{aligned} m_1 &= 7, & m_2 &= 8, \\ l_1 &= \frac{1}{2}, & l_2 &= \frac{3}{4}. \end{aligned}$$

We again assumed quadratic cost 16 with $Q = R = I$. However, the tracking cost was chosen as $Q_{\text{LQR}} = 1000I$ to obtain suitable tracking performance. One interesting remark to mention is the fact that elements of the gain matrix K of the linearized model around the equilibrium are quite large

$$K = -1000 \cdot (1.58 \quad 0.70 \quad 0.52 \quad 0.26)$$

and thus we chose the norm tolerance ϵ_0 where the control is switched to the LQR regulation as 10^{-5} . Also we set the time step of demonstrations to 0.01 to achieve sufficiently accurate tracking. We chose the set where we want the stabilizing controller as $D = [-0.15, 0.15]^4$ and we set the minimum target trajectory switch time to 1.5, the maximum time span of the demonstrations as 8 seconds, and γ as 0.01.

A polynomial of the 4th order (with even powers only, $P = [-100, 100]^{45}$) was enough to find a suitable candidate and 67 trajectories were added during the run of the algorithm. The control was accepted after 200000 subsequent successful simulations. The time required for the whole run of the algorithm was 10169 seconds.

$$\begin{aligned} L &= 85.335\theta_1\theta_2 + 83.130\theta_1\dot{\theta}_1 + 42.601\theta_1\dot{\theta}_2 + 4.332\theta_2^4 + 2.693\theta_2^3\dot{\theta}_2 + \\ &+ 20.117\theta_2^2 - 2.278\theta_2\dot{\theta}_1^2\dot{\theta}_2 + 41.777\theta_2\dot{\theta}_1 + 0.23975\theta_2\dot{\theta}_2^3 + 21.397\theta_2\dot{\theta}_2 - \\ &- 16.102\dot{\theta}_1^2\dot{\theta}_2^2 + 64.656\dot{\theta}_1^2 + 22.669\dot{\theta}_1\dot{\theta}_2^3 + 65.411\dot{\theta}_1\dot{\theta}_2 + 15.862\dot{\theta}_2^4 + \\ &+ 16.564\dot{\theta}_2^2 \end{aligned}$$

We can again compare the algorithm with the simulation only approach. The simulations in the simulation-only approach took 10996 seconds, with added 12 trajectories. If we look at the last successful run of the falsifier, it is 8723s (simulation only) versus 3981s (Lyapunov). Again, the difference is quite noticeable. However, this difference could be even bigger if it was not for the fact that the stabilizing trajectories leave the set D considerably (see Figure 13). Finally, we provide a comparison of the cost of the gained LQR switching controller on D with the cost of the LQR controller around the equilibrium which for the most

# parameters of L	45
# counterexamples (positive definiteness)	6
# counterexamples (decrease condition)	67
# demonstrations	67
# states in all demonstrations	31894
# inequalities	1569
Demonstrator time	375.7s
Learner time	2667.3s
Falsifier (positive definiteness) time	226.6s
Falsifier (decrease condition) time	6786.2s
Falsifier (decrease condition) simulations	521260
Total time	10169s

Table 5: The run of the algorithm for the acrobot example

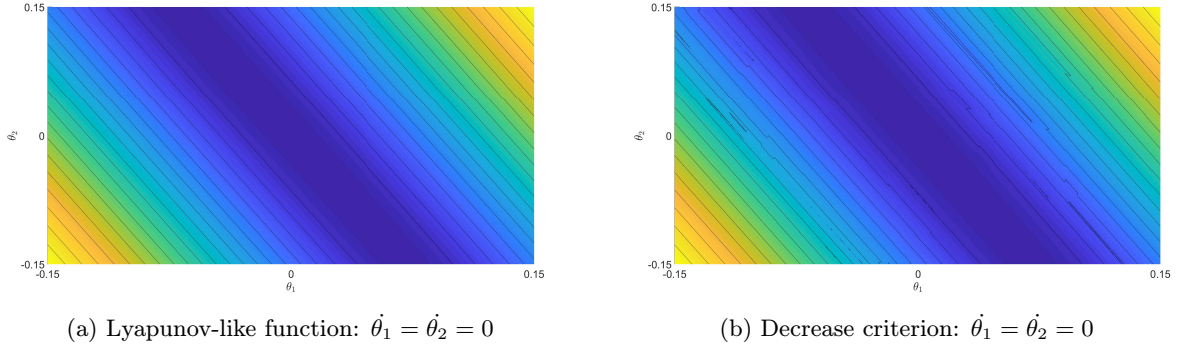


Figure 12: Acrobot: polynomial (4th order) Lyapunov-like function compatible with the learned control for the acrobot

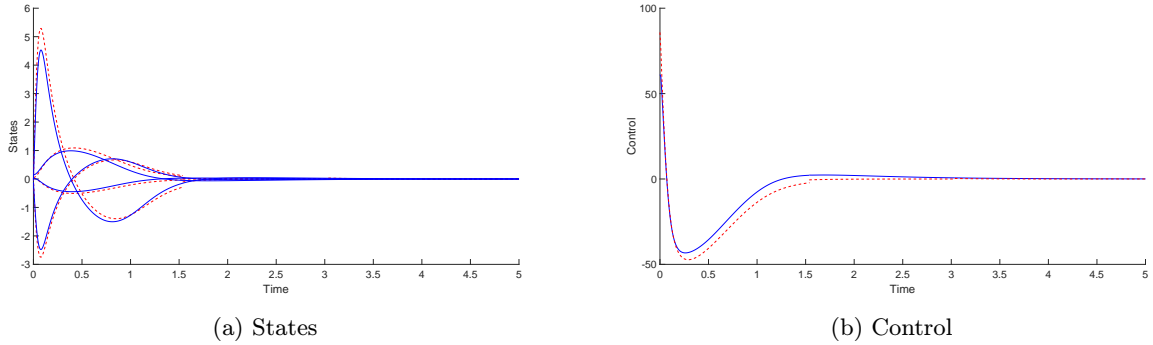


Figure 13: Acrobot: LQR switching control trajectory, red dashed line denotes target trajectories

part stabilizes the system (we do not give a comparison with Sontag’s formula again due to the expansive nature of the system that translates to the requirement of finding a CLF on a much larger set than D to generate a control law that stabilizes the system on D).

6.5 Example 5: Caltech ducted fan

We assume the planar model of a fan in hover mode

$$\begin{aligned}
 m\ddot{x} &= -d_c\dot{x} + u_1 \cos \theta - u_2 \sin \theta \\
 m\ddot{y} &= -d_c\dot{y} + u_2 \cos \theta + u_1 \sin \theta - mg \\
 J\ddot{\theta} &= ru_1,
 \end{aligned} \tag{21}$$

where $m = 11.2$, $g = 0.28$, $J = 0.0462$, $r = 0.156$ and $d_c = 0.1$. The variables x and y denote the position of the centre of the mass of the fan (y denotes the height), θ is the orientation of the fan, J is its moment of the

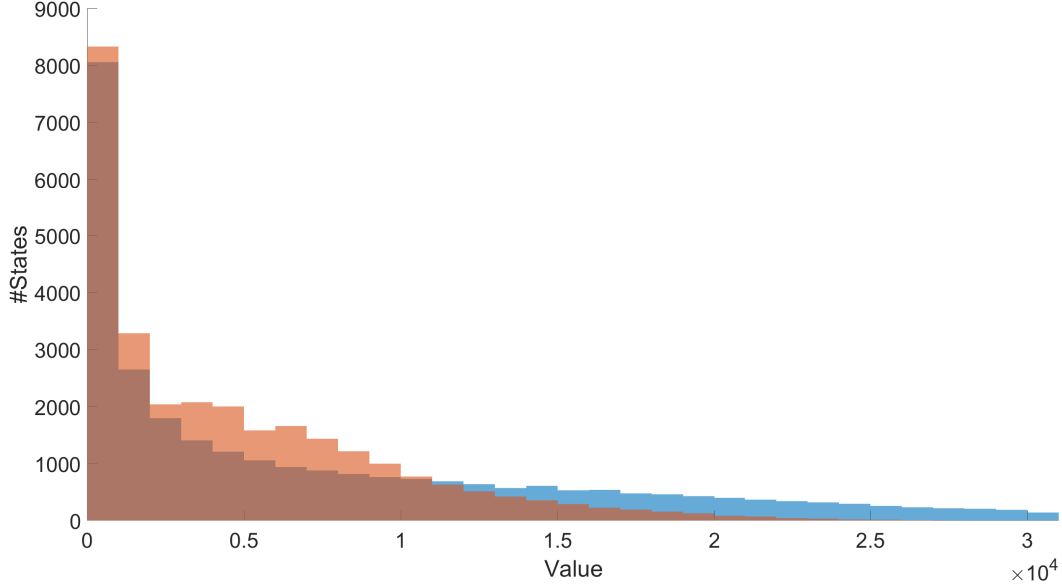


Figure 14: Acrobot: value of LQR around the equilibrium (blue, mean value is 7675) and the LQR switching control (red, mean value is 4698)

# parameters of L	21
# counterexamples (positive definiteness)	10
# counterexamples (decrease condition)	73
# demonstrations	73
# states in all demonstrations	35149
# added inequalities	1042
Demonstrator time	161.0s
Learner time	568.2s
Falsifier (positive definiteness) time	328.9s
Falsifier (decrease condition) time	5803s
Falsifier (decrease condition) simulations	907696
Total time	6972s

Table 6: The run of the algorithm for the fan example

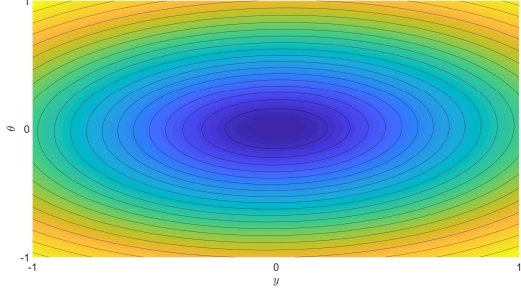
inertia, d_c is the friction coefficient, m is its mass of the fan, u_1 denotes the force perpendicular to the axis of the fan and u_2 is the force that is parallel, both acting at the distance r from the centre of the mass of the fan [18].

We again used the quadratic cost (16) with $Q = R = I$ (the cost of LQR tracking is also the same) and set the tolerance ϵ_0 where the control is switched to LQR around the equilibrium to 0.01. We use demonstrations that are 40 seconds long, with the time step of the demonstrator being 0.05. The investigated set was chosen as $D = [-1, 1]^6$, γ as 0.01, and the minimum target trajectory switch time as $t_{\min} = 1.5s$. For $P = [-100, 100]^{21}$, the quadratic candidate

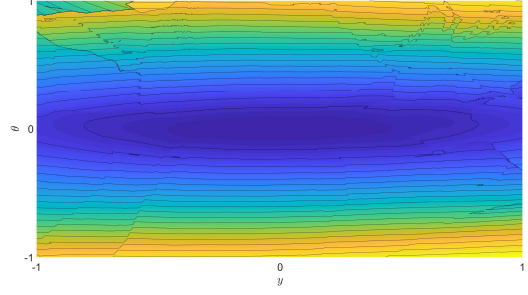
$$\begin{aligned}
 L = & 9.591x^2 + 1.424xy - 7.087x\theta + 19.822x\dot{x} + 5.497x\dot{y} - 1.636x\dot{\theta} + 2.318y^2 - 0.215y\theta + \\
 & + 0.6208y\dot{x} + 1.588y\dot{y} - 0.113y\dot{\theta} + 4.217\theta^2 - 16.116\theta\dot{x} - 2.128\theta\dot{y} + 2.331\theta\dot{\theta} + \\
 & + 47.061\dot{x}^2 + 8.411\dot{x}\dot{y} - 5.203\dot{x}\dot{\theta} + 40.935\dot{y}^2 - 0.279\dot{y}\dot{\theta} + 0.399\dot{\theta}^2
 \end{aligned}$$

was found after adding 73 trajectories. The whole run took 6972s, where the control law was accepted after successful 200000 simulations.

We also provide a cost comparison with Sontag's formula (14) on $[-0.5, 0.5]^6$, using the learned quadratic

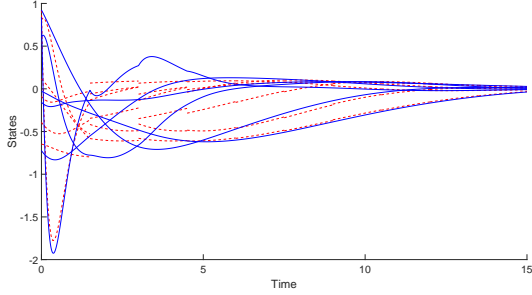


(a) Lyapunov function: $x = \dot{x} = \dot{y} = \dot{\theta}$

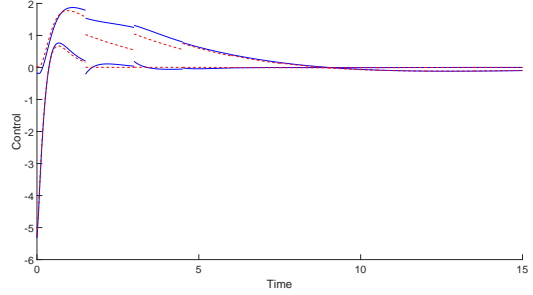


(b) Decrease criterion: $x = \dot{x} = \dot{y} = \dot{\theta}$

Figure 15: Fan: quadratic Lyapunov-like function compatible with the learned control for the fan



(a) States



(b) Control

Figure 16: Fan: LQR switching control trajectory, red dashed line denotes target trajectories

CLF

$$\begin{aligned}
 L = & 9.241x^2 + 0.759xy - 10.022x\theta + 29.314x\dot{x} + 8.172x\dot{y} - 2.659x\dot{\theta} + 4.519y^2 - 0.248y\theta - \\
 & - 1.020y\dot{x} + 9.036y\dot{y} + 0.402y\dot{\theta} + 6.635\theta^2 - 27.597\theta\dot{x} - 2.791\theta\dot{y} + 4.030\theta\dot{\theta} + \\
 & + 47.312\dot{x}^2 + 12.093\dot{x}\dot{y} - 10.604\dot{x}\dot{\theta} + 34.910\dot{y}^2 - 0.861\dot{y}\dot{\theta} + 1.168\dot{\theta}^2.
 \end{aligned}$$

Finally, we ran the simulation only approach. The simulations in the simulation-only approach took 7337s, adding 12 trajectories, and the last successful run of the falsifier took 4273s in comparison to 1290s of the Lyapunov based approach.

6.6 Example 6: Quadcopter

Let us consider a problem in slightly higher dimensions. We assume the quadcopter model

$$\begin{aligned}
 m\ddot{x} &= u_1(\sin\phi\sin\psi + \cos\phi\cos\psi\sin\theta) \\
 m\ddot{y} &= u_1(\cos\phi\sin\theta\sin\psi - \cos\psi\sin\phi) \\
 m\ddot{y} &= u_1\cos\theta\cos\phi - mg \\
 m\ddot{\psi} &= u_2 \\
 m\ddot{\theta} &= u_3 \\
 m\ddot{\phi} &= u_4.
 \end{aligned} \tag{22}$$

with quadratic cost (16) for $Q = R = I$ (the same as the cost of the used LQR tracking).

First, we considered the set $D = [-1, 1]^{12}$ with $S = [-10, 10]^{12}$, and we set $\epsilon_0 = 0.01$, $\gamma = 0.01$, and $t_{\min} = 1$. Demonstrations were 10 seconds long with a time step of 0.05. A quadratic polynomial candidate

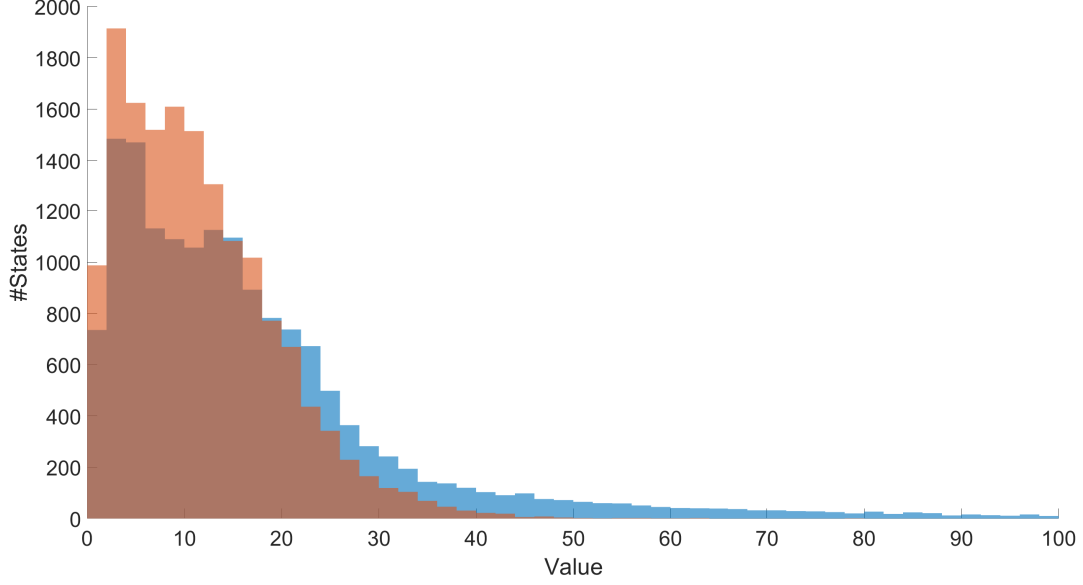


Figure 17: Fan: value of Sontag's formula (blue, mean value is 18.4) and the LQR switching control (red, mean value is 11.6)

was sufficient for this setup ($P = [-100, 100]^{78}$). We found the result

$$\begin{aligned}
L = & 3.450x^2 - 2.457xy + 5.741xz + 0.231x\phi - 3.018x\psi + 9.119x\theta + 3.116x\dot{x} + 1.108x\dot{y} + 3.505x\dot{z} - \\
& - 2.754x\dot{\phi} - 1.243x\dot{\psi} - 0.943x\dot{\theta} + 4.935y^2 + 2.361yz - 18.798y\phi - 10.064y\psi - 6.449y\theta + 0.928y\dot{x} + \\
& + 3.809y\dot{y} + 0.483y\dot{z} - 1.416y\dot{\phi} - 5.876y\dot{\psi} + 2.438y\dot{\theta} + 15.587z^2 - 7.303z\phi - 18.477z\psi + \\
& + 4.682z\theta - 2.040z\dot{x} - 3.7334z\dot{y} + 10.078z\dot{z} + 3.427z\dot{\phi} + 0.001z\dot{\psi} - 2.436z\dot{\theta} + 97.742\phi^2 + \\
& + 22.628\phi\psi + 18.888\phi\theta - 9.006\phi\dot{x} - 20.905\phi\dot{y} + 6.422\phi\dot{z} + 37.618\phi\dot{\phi} - 12.402\phi\dot{\psi} - \\
& - 4.857\phi\dot{\theta} + 84.238\psi^2 + 5.952\psi\theta + 1.976\psi\dot{x} + 0.156\psi\dot{y} + 0.272\psi\dot{z} + 3.856\psi\dot{\phi} + \\
& + 39.684\psi\dot{\psi} + 0.531\psi\dot{\theta} + 97.742\theta^2 + 32.264\theta\dot{x} - 3.445\theta\dot{y} + 4.141\theta\dot{z} + 6.366\theta\dot{\phi} - \\
& - 22.0\theta\dot{\psi} + 41.178\theta\dot{\theta} + 5.1505\dot{x}^2 + 0.93925\dot{x}\dot{y} + 2.6872\dot{x}\dot{z} - 0.73247\dot{x}\dot{\phi} - \\
& - 19.549\dot{x}\dot{\psi} + 9.474\dot{x}\dot{\theta} + 7.064\dot{y}^2 - 4.533\dot{y}\dot{z} - 15.665\dot{y}\dot{\phi} - 5.585\dot{y}\dot{\psi} + \\
& + 0.571\dot{y}\dot{\theta} + 9.099\dot{z}^2 + 1.447\dot{z}\dot{\phi} - 4.352\dot{z}\dot{\psi} + 3.367\dot{z}\dot{\theta} + 14.492\dot{\phi}^2 - \\
& - 5.550\dot{\phi}\dot{\psi} + 0.004\dot{\phi}\dot{\theta} + 97.742\dot{\psi}^2 - 11.484\dot{\psi}\dot{\theta} + 8.626\dot{\theta}^2
\end{aligned}$$

after 1000000 successful simulations. Note that in this example we used a linear programming learner based on the Chebyshev center [34] instead of a semidefinite programming learner based on the maximum volume ellipsoid, in order to save computation time.

It should be noted that on $[-1, 1]^{12}$, the quadcopter system is mostly (we detected 6 counterexamples in 100000 random samples due to leaving S) stabilizable by its LQR around the equilibrium. However, adding more trajectories (136 in this examples) leads to a significant decrease of cost as seen in the cost comparison based on 100000 samples.

Next, we increased the set D to $D = [-1.5, 1.5]^{12}$, to see how this influences the algorithm. We choose to stop it when 500000 subsequent simulations were successful. As can be seen from Figure 21 that describes the number of simulations during the run of the algorithm, this increases the number of required trajectories significantly. Still, if we investigate the number of added demonstrations to the dimensions of the problem, we still get quite a poor resolution (468878 total number of points, i.e. $462422^{\frac{1}{12}} \approx 3$ grid points per dimension).

We also observe the noticeable increasing trend of required simulations to find a new counterexample as the number of demonstrations increases, see Figure 21. Of course, this dependence is not monotonous, due to randomness and due to the fact that sometimes adding a new trajectory can increase the number of counterexamples. In Figure 21, we can also see how the used candidate stabilizes during the run. It should be noted however, that the total number of simulations during this run is 61.8 millions which corresponds to

# parameters of L	78
# counterexamples (positive definiteness)	692
# counterexamples (decrease condition)	136
# demonstrations	136
# states in all demonstrations	35149
# added inequalities	1811
Demonstrator time	524.0s
Learner time	129.8s
Falsifier (positive definiteness) time	2683.1s
Falsifier (decrease condition) time	95300s
Falsifier (decrease condition) simulations	11176683
Total time	98803s

Table 7: The run of the algorithm for the quadcopter example

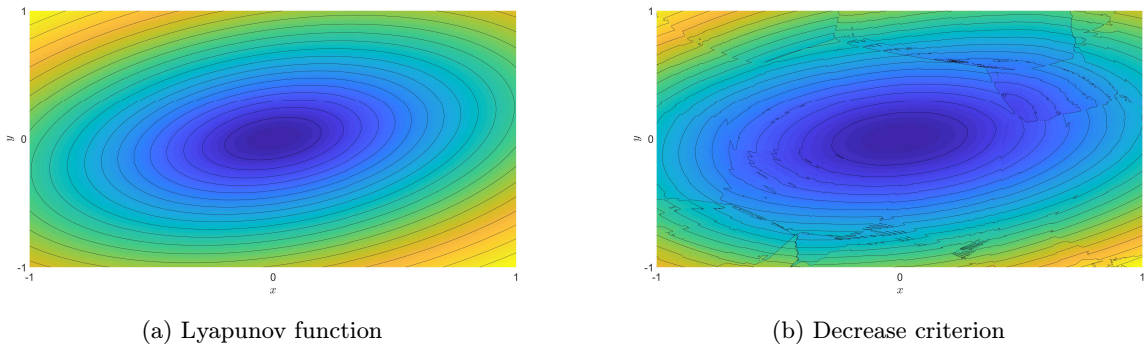


Figure 18: Quadcopter: quadratic Lyapunov-like function compatible with the learned control for the quadcopter

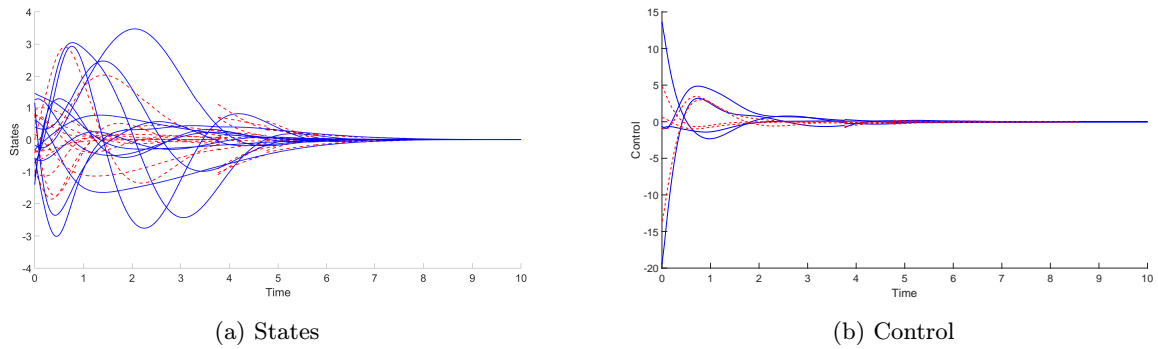


Figure 19: Quadcopter: LQR switching control trajectory, red dashed line denotes target trajectories

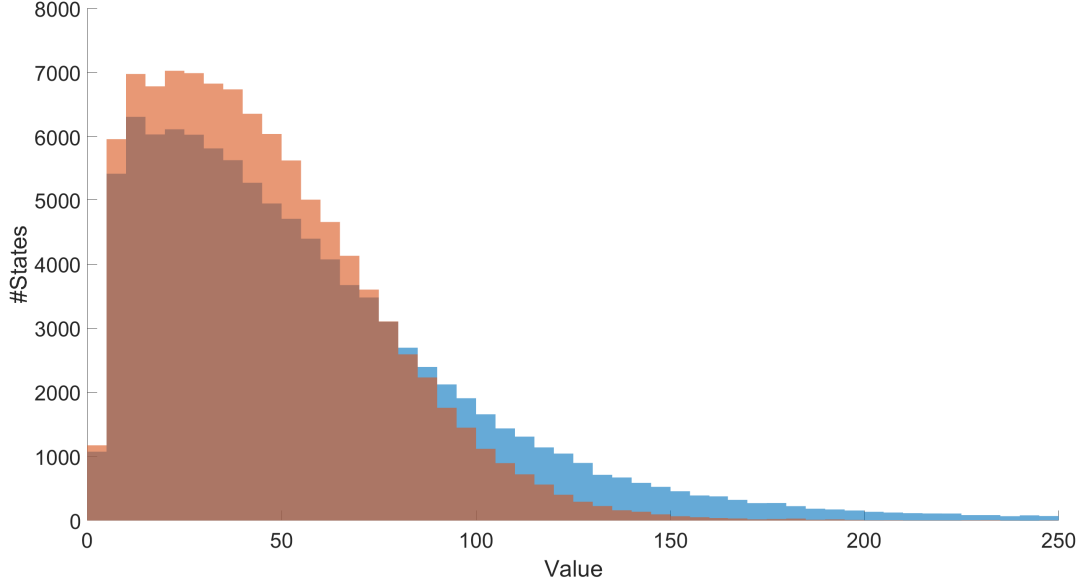


Figure 20: Quadcopter: value of LQR around the equilibrium (blue, mean value is 59.7) and the LQR switching control (red, mean value is 46.0)

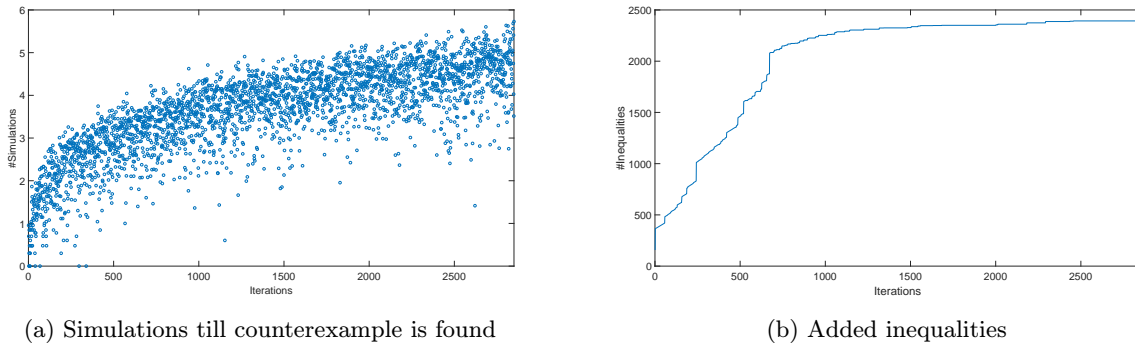


Figure 21: Quadcopter: the run of the algorithm for $D = [-1.5, 1.5]^{12}$

approximately 206 hours of computation time. This clearly shows the limitation the implementation based on pure sampling. Still, the total number of demonstrations is much more reasonable and shows that this method of constructing control laws has promise with a more efficient falsifier/verifier.

7 Discussion

We conclude this text with various observations we made in implementing the proposed algorithm and discuss possible extensions of the proposed algorithm to increase its efficiency.

Formal verification

The fact that our approach does not only produce a feedback control law, but also a corresponding Lyapunov function, opens the possibility of formal verification of stability [12, 1]. While the formal verification of Definition 5 still needs a rigorous ODE solver [29], as discussed at the end of Section 4.3.2 our algorithm will eventually produce a Lyapunov-like function that can be formally verified by purely algebraic solvers.

Selection of candidates

In our implementation, we have selected candidates as centres of maximum volume ellipsoids. The motivation behind this selection lies in the guaranteed decrease of the admissible parameter space [34, 42]

$$V_{\text{new}} \leq \alpha V_{\text{old}}.$$

However from our experience, the candidate selection became a significant computational burden for high dimensional problems with non-quadratic polynomial candidates. An attractive variant is the Chebyshev centre which requires solving a linear program (in comparison to a semidefinite program needed for a centre of maximum volume ellipsoid) that offers significantly better scalability. However, for the Chebyshev centre we do not know of any similar inequality granting a guaranteed decrease [34].

Other systems of candidates

Our learning framework is built for linearly parametrised systems of candidates, where polynomials present a natural candidate for Lyapunov-like functions. However, there are nonlinear system for which no polynomial CLF exists [4, 3]. The extension to other function approximations like neural networks is in this case quite obvious [12]. However, the issue of finding suitable candidates may deepen in this case.

Expanding the investigated set

We have seen in the fourth example (acrobot) that the stabilizing control may leave the investigated set significantly. This phenomenon can severely decrease the performance of the algorithm, turning it mostly into the pure simulation approach. The solution could be to increase the investigated set dynamically. This would allow to fully eliminate the simulations outside of the set, where the Lyapunov candidate is defined.

Local CLFs

We have tried to learn a CLF compatible with demonstrator. However, it may not be possible to find a single one for more complicated systems. A natural extension of our algorithm is to learn multiple Lyapunov functions each belonging to one trajectory [43, 33]. The noteworthy complication that is brought with CLFs for path tracking is the fact that they are generally time-dependent (since the tracking model itself varies in time). Moreover, the algorithm would have to decide in each iteration whether to add a new trajectory or to modify the CLF for the current trajectory in order to handle the founded counterexample.

Finding counterexamples

Our implementation is driven by uniform random sampling to detect possible counterexamples. This is perfectly fine for a simulation-only approach, in which we de facto optimize a zero-one function. However, the knowledge of such a candidate offers the possibility of using more advanced falsifiers. For example, there is a clear optimization criterion in the form of the difference of the values of the Lyapunov candidate at the beginning and at the end. Hence, it may be possible to find counterexamples using a global optimization algorithm. But it should be noted that the optimized function in question is discontinuous by definition.

Non-LQR control laws

Although we concretized the generic algorithm from Section 3 using LQR tracking, it is not restricted to this particular choice. LQR control laws are attractive due to their ease of construction, but they limit the usage to systems for which LQR is properly defined and does not allow to use learned CLF candidates to directly participate in controller synthesis, which would, for example, be possible using certain MPC approaches [32]. However, even the widely used PID control would be a possible alternative.

8 Conclusion

We have proposed a framework for learning control Lyapunov functions and synthesizing control laws that inherits optimality with respect to a chosen cost functional from the given demonstrator. We have stated a specific LQR variant of the given framework and provided some asymptotic guarantees. We have also implemented the algorithm and tested it on various case studies. We have made a comparison in terms of cost between our synthesised control law and Sontag’s formula and observed significant cost decrease. We have also made a time comparison with a simulation-only approach and have seen significant time savings in learning Lyapunov functions.

References

- [1] A. Abate, D. Ahmed, M. Giacobbe, and A. Peruffo. Formal synthesis of Lyapunov neural networks. *IEEE Control Systems Letters*, 5(3):773–778, 2020.

- [2] D. Aeyels and J. Peuteman. A new asymptotic stability criterion for nonlinear time-variant differential equations. *IEEE Transactions on Automatic Control*, 43(7):968–971, 1998.
- [3] A. A. Ahmadi and B. E. Khadir. A globally asymptotically stable polynomial vector field with rational coefficients and no local polynomial Lyapunov function. *Systems & Control Letters*, 121(4):50–53, 2018.
- [4] A. A. Ahmadi, M. Krstic, and P. A. Parrilo. A globally asymptotically stable polynomial vector field with no polynomial Lyapunov function. *50th IEEE Conference on Decision and Control and European Control Conference*, pages 7579–7580, 2011.
- [5] J. A. E. Andersson, J. Gillis, G. Horn, James B Rawlings, and Moritz Diehl. CasADi – A software framework for nonlinear optimization and optimal control. *Mathematical Programming Computation*, 11(1), 2018.
- [6] C. W. Barrett, R. Sebastiani, S. A. Seshia, and C. Tinelli. Satisfiability modulo theories. In *Handbook of Satisfiability*, volume 185, pages 825–885. 2009.
- [7] R. W. Beard, G. N. Saridis, and J. T. Wen. Galerkin approximations of the generalized Hamilton-Jacobi-Bellman equation. *Automatica*, 33(12):2159–2177, 1997.
- [8] D. P. Bertsekas. *Dynamic Programming and Optimal Control*. Athena Scientific, 2005.
- [9] J. T. Betts. *Practical Methods for Optimal Control and Estimation Using Nonlinear Programming*. SIAM, 2010.
- [10] S. Boyd and L. Vandenberghe. *Convex Optimization*. Cambridge University Press, 2004.
- [11] R. T. Bupp, D. S. Bernstein, and V. T. Coppola. A benchmark problem for nonlinear control design. *International Journal of Robust and Nonlinear Control*, 8(4-5):307–310, 1998.
- [12] Y. Chang, N. Roohi, and S. Gao. Neural Lyapunov control. In H. Wallach, H. Larochelle, A. Beygelzimer, F. d'Alché-Buc, E. Fox, and R. Garnett, editors, *Advances in Neural Information Processing Systems*, volume 32, pages 3245–3254. Curran Associates, Inc., 2019.
- [13] R. A. Freeman and P. V. Kokotovic. Inverse optimality in robust stabilization. *SIAM Journal on Control and Optimization*, 34(4):1365–1391, 1996.
- [14] R. A. Freeman and P. V. Kokotovic. *Robust Nonlinear Control Design*. Birkhäuser Boston, 1996.
- [15] R. A. Freeman and J. A. Primbs. Control Lyapunov functions: new ideas from an old source. *Proceedings of 35th IEEE Conference on Decision and Control*, 4:3926–3931, 1996.
- [16] E. Hairer, S. P. Norsett, and G. Wanner. *Solving Ordinary Differential Equations I*. Springer, 1993.
- [17] C. R. Hargraves and S. W. Paris. Direct trajectory optimization using nonlinear programming and collocation. *Journal of Guidance, Control, and Dynamics*, 10(4):338–342, 1987.
- [18] A. Jadbabaie and J. Hauser. Control of a thrust-vectoring flying wing: A receding horizon-LPV approach. *International Journal of Robust and Nonlinear Control*, 12(9):869–896, 2002.
- [19] R. E. Kalman. Contribution to the theory of optimal control. *Bol. Soc. Mat. Mexicana*, 5, 1960.
- [20] H. K. Khalil. *Nonlinear Systems*. Prentice Hall, 3rd edition, 2002.
- [21] S. M. Khansari-Zadeh and A. K. Billard. Learning control Lyapunov function to ensure stability of dynamical system based robot reaching motions. *Robotics and Autonomous Systems*, 62(6):752–765, 2007.
- [22] H. Kwakernaak and R. Sivan. *Linear Optimal Control Systems*, volume 1. Wiley-interscience New York, 1972.
- [23] S. M. LaValle. *Planning algorithms*. Cambridge University Press, 2006.
- [24] F. L. Lewis, D. L. Vrabie, and V. S. Syrmos. *Optimal control, third edition*. John Wiley, 2012.
- [25] D. Liberzon. *Calculus of Variations and Optimal Control Theory: A Concise Introduction*. Princeton University Press, New Jersey, 2011.

- [26] J. Löfberg. YALMIP : A toolbox for modeling and optimization in MATLAB. In *In Proceedings of the CACSD Conference*, Taipei, Taiwan, 2004.
- [27] I. Mordatch and E. Todorov. Combining the benefits of function approximation and trajectory optimization. In *Robotics: Science and Systems*, volume 4, 2014.
- [28] R. M. Murray and J. Hausser. A case study in approximate linearization: The acrobot example. *Technical report, UC Berkeley, EECS Department*, 1991.
- [29] N. S. Nedialkov, K. R. Jackson, and G. F. Corliss. Validated solutions of initial value problems for ordinary differential equations. *Appl. Math. Comput.*, 105:21–68, 1999.
- [30] I. Noreen, A. Khan, and Z. Habib. Optimal path planning using RRT* based approaches: A survey and future directions. *International Journal of Advanced Computer Science and Applications*, 7(11), 2016.
- [31] K. Price, R. M. Storn, and J. A. Lampinen. *Differential Evolution: A Practical Approach to Global Optimization*. Springer-Verlag Berlin Heidelberg, 2005.
- [32] J. A. Primbs, V. Nevistic, and J. C. Doyle. Nonlinear optimal control: A control Lyapunov function and receding horizon perspective. *Asian Journal of Control*, 1:14–24, 1999.
- [33] H. Ravanbakhsh, S. Aghli, C. Heckman, and S. Sankaranarayanan. Path-following through control funnel functions. *EEE/RSJ International Conference on Intelligent Robots and System*, pages 401–408, 2018.
- [34] H. Ravanbakhsh and S. Sankaranarayanan. Learning control Lyapunov functions from counterexamples and demonstrations. *Autonomous Robots*, 43(2):275–307, 2019.
- [35] H. Ravichandar, A. Polydoros, S. Sonia, and A. Billard. Recent advances in robot learning from demonstration. *Annual Review of Control, Robotics, and Autonomous Systems*, 3, 2020.
- [36] P. Reist, P. Preiswerk, and R. Tedrake. Feedback-motion-planning with simulation-based LQR-trees. *The International Journal of Robotics Research*, 35(11):1393–1416, 2016.
- [37] R. Sepulchre, M. Jankovic, and P. V. Kokotovic. *Constructive Nonlinear Control*. Springer-Verlag London, 1997.
- [38] E. D. Sontag. A characterization of asymptotic controllability. *Dynamical systems II (Proceedings of University of Florida international symposium)*, pages 645–648, 1982.
- [39] E. D. Sontag. A ‘universal’ construction of Artstein’s theorem on nonlinear stabilization. *Systems & Control Letters*, 13:117–123, 1989.
- [40] E. D. Sontag. *Mathematical Control Theory*. Springer-Verlag New York, 1998.
- [41] W. Tan and A. Packard. Searching for control Lyapunov functions using sums of squares programming. *Allerton conference on communication, control and computing*, pages 210–219, 2004.
- [42] S. Tarasov, L. Khachian, and I. Erlikh. The method of inscribed ellipsoids. *Doklady Akademii Nauk SSSR*, 298(5):1081–1085, 1988.
- [43] R. Tedrake, I. R. Manchester, M. Tobenkin, and J. W. Roberts. LQR-trees: Feedback motion planning via sums-of-squares verification. *The International Journal of Robotics Research*, 29(8):1038–1052, 2010.
- [44] K.C. Toh, M.J. Todd, and R.H. Tutuncu. SDPT3—a Matlab software package for semidefinite programming. *Optimization Methods and Software*, 11:545–581, 1999.
- [45] U. Topcu, A. Packard, P. Seiler, and T. Wheeler. Stability region analysis using simulations and sum-of-squares programming. *Proceedings of the American control conference*, pages 6009–6014, 2007.
- [46] MATLAB version 9.5 (R2018b). The MathWorks Inc., Natick, Massachusetts, 2018.
- [47] A. Wächter and L. T. Biegler. On the implementation of a primal-dual interior point filter line search algorithm for large-scale nonlinear programming. *Mathematical Programming*, 106(1):25–57, 2006.

A Appendix

A.1 Proofs of the Properties of LQR Tracking

We start with the proof of uniform continuity of LQR tracking. We assume system (1) and assume that set D of all initial points of all possible demonstrations is compact. In addition, we also assume that all demonstrations are of length T , and are continuous as a function of their initial states. Then the following proposition holds.

Proposition 1. *Every LQR tracking trajectory $\Sigma(x_0, u_{\text{LQR}}^{(\tilde{x}, \tilde{u})}) : [0, T] \rightarrow \mathbb{R}^n$ is, as a function of time, its initial state x_0 and the initial state $\tilde{x}(0)$ of its target trajectory \tilde{x} uniformly continuous on $[0, T] \times D \times D$.*

Proof. Let us denote the LQR tracking trajectory $\Sigma(x_0, u_{\text{LQR}}^{(\tilde{x}, \tilde{u})})$ simply as x and note that it is a function of time, its initial state and the initial state of its target trajectory. We first observe that x is a solution to the ODE

$$\begin{aligned} \dot{x} &= f(x, \tilde{u}(t, \tilde{x}(0)) - K(t, \tilde{x}(0)) [x - \tilde{x}(t, \tilde{x}(0))]) \\ x(0) &= x_0, \end{aligned} \quad (23)$$

where the functions $\tilde{x}(t, \tilde{x}(0))$ and $\tilde{u}(t, \tilde{x}(0))$ denote the states and the controls of the target trajectory that is assigned to x_0 , and where $K(t, \tilde{x}(0))$ is the solution of the Riccati equation that corresponds to the LQR tracking problem.

We will first show that x depends on x_0 and $\tilde{x}(0)$ continuously. Let us interpret $\tilde{x}(0)$ as a specific value of some parameter λ

$$\dot{x} = f(x, \tilde{u}(t, \lambda) - K(t, \lambda) [x - \tilde{x}(t, \lambda)]) \quad (24)$$

$$x(0) = x_0 \quad (25)$$

$$\lambda = \tilde{x}(0).$$

We know that $\tilde{u}(t, \lambda)$ and $\tilde{x}(t, \lambda)$ are jointly continuous in both t and λ . Moreover,

$$K(t, \lambda) = -R_{\text{LQR}}^{-1} B(\tilde{x}(t, \lambda), \tilde{u}(t, \lambda))^T S(t, \lambda)$$

is obtained from a solution of the Riccati equation

$$-\dot{S} = Q_{\text{LQR}} - S B(\tilde{x}(t, \lambda), \tilde{u}(t, \lambda)) R_{\text{LQR}}^{-1} B(\tilde{x}(t, \lambda), \tilde{u}(t, \lambda))^T S + S A(\tilde{x}(t, \lambda), \tilde{u}(t, \lambda)) + A(\tilde{x}(t, \lambda), \tilde{u}(t, \lambda))^T S \quad (26)$$

$$S(t_{\text{traj}}) = Q_{\text{LQR}},$$

where $A(x, u) = \frac{\partial f(x, u)}{\partial x}$, $B(x, u) = \frac{\partial f(x, u)}{\partial u}$, and Q_{LQR} and R_{LQR} are some fixed positive definite matrices. Since both A and B are smooth and both $\tilde{x}(t, \lambda)$, $\tilde{u}(t, \lambda)$ are continuous in λ , a solution $S(t, \lambda)$ is continuous in parameter λ on D uniformly for $t \in [0, T]$ due to [20, Theorem 3.5] and consequently, $K(t, \lambda)$ is jointly continuous in t and λ .

Hence, if we combine all combined together, the right hand side of (24) is jointly continuous in x , t and λ . Additionally, since f is smooth, it is locally Lipschitz in x uniformly for $t \in [0, T]$ and $\lambda \in D$. Hence, the solution x is jointly continuous in both x_0 and λ uniformly in $t \in [0, T]$ due to [20, Theorem 3.5]. This together with the continuity of x in t , implies joint continuity of x in all three arguments.

We showed that x is continuous in all three arguments. Moreover the set of the allowed values t, x_0 and λ is compact. Thus, the solution x is uniformly continuous on $[0, T] \times D \times D$. \square

Next, we move to the cost of LQR tracking, if an initial point of LQR tracking is near a target trajectory.

Proposition 2. *Let (\tilde{x}, \tilde{u}) be a continuous trajectory of length T . Then for all $t \in [0, T]$,*

$$\left| \text{cost}_{V_i}(x_0, u_{\text{LQR}}^{(\tilde{x}, \tilde{u})}) - \text{cost}_{V_i}(\tilde{x}(0), \tilde{u}) \right| \rightarrow 0$$

as $x_0 \rightarrow \tilde{x}(0)$.

Proof. Due to Proposition 1, the LQR tracking state trajectory $\Sigma(x_0, u_{\text{LQR}}^{(\tilde{x}, \tilde{u})})$ is continuous with respect to its initial state x_0 and the initial state of the tracked trajectory $\tilde{x}(0)$. Let us denote $\Sigma(x_0, u_{\text{LQR}}^{(\tilde{x}, \tilde{u})})$ simply as

x . Using continuity of x , for any $\varepsilon' > 0$, there is a neighbourhood H' of $\tilde{x}(0)$ such that for any $x_0 \in H'$ and for all $t \in [0, T]$

$$\|x(t) - \tilde{x}(t)\| < \varepsilon'.$$

Also since we considered a demonstrator that provides control laws \tilde{u} continuous with respect to initial states and since the LQR tracking control is

$$u(t) = \tilde{u}(t) - K(\tilde{x}(0), t)(x(t) - \tilde{x}(t)),$$

where $K(\tilde{x}(0), t)$ is continuous, for any $\varepsilon'' > 0$, there is a neighbourhood H' of $\tilde{x}(0)$ such that for any $x_0 \in H'$ and for all $t \in [0, T]$

$$\|u(t) - \tilde{u}(t)\| < \varepsilon''.$$

If we put both of these observations together, we can find a neighbourhood H of $\tilde{x}(0)$ such that for any $x_0 \in H$ and for all $t \in [0, T]$

$$\|(x(t), u(t)) - (\tilde{x}(t), \tilde{u}(t))\| < \varepsilon.$$

Using Taylor expansion of Q and R , we get for the cost of LQR tracking

$$\text{cost}_{V_t}(x_0, u_{\text{LQR}}^{\tilde{x}, \tilde{u}}) = \int_0^t Q(x(\tau)) + R(u(\tau)) d\tau = \int_0^t Q(\tilde{x}(\tau)) + R(\tilde{u}(\tau)) d\tau + \int_0^t r(x(\tau), u(\tau)) d\tau,$$

where $r(x(\tau), u(\tau))$ is a remainder in the Taylor formula which can be written in the Lagrange form as

$$r(x(\tau), u(\tau)) = \nabla(Q(x) + R(u))|_{y=(\tilde{y}(\tau)+c(\tau)(y(\tau)-\tilde{y}(\tau)))}(y - \tilde{y}),$$

where $c(\tau) \in [0, 1]$ and $y(\tau) = (x(\tau), u(\tau))^T$. Since $\tilde{y}(\tau)$ is contained in bounded open set S (see Definition 1 of a continuous demonstrator), $y(\tau)$ can be contained in the compact set \tilde{S} for ε small enough. In addition, the functions Q and R are smooth. Hence, we can estimate the remainder as

$$\|r(x(\tau), u(\tau))\| \leq C\varepsilon$$

for some $C > 0$ and hence

$$\left| \text{cost}_{V_t}(x_0, u_{\text{LQR}}^{\tilde{x}, \tilde{u}}) - \text{cost}_{V_t}(\tilde{x}(0), \tilde{u}) \right| \leq Ct\varepsilon.$$

Thus, the cost of the LQR tracking trajectory tends to the demonstrator's cost as the initial points tends to each other. \square

The result extends to the switching control from Definition 4 as well.

Proposition 3. *Let (\tilde{x}, \tilde{u}) be a continuous trajectory of length T . For every LQR switching control law $u_{\text{switch}}^{\mathcal{T}}$ based on a set of demonstrations \mathcal{T} , an assignment rule ϕ dominated by the Euclidean metric, and $t_{\min} > 0$, for all $t \in [0, T]$,*

$$\left| \text{cost}_{V_t}(x_0, u_{\text{switch}}^{\mathcal{T}}) - \text{cost}_{V_t}(\tilde{x}(0), \tilde{u}) \right| \rightarrow 0$$

as $x_0 \rightarrow \tilde{x}(0)$.

Proof. Let $0 < t \leq T$ and consider the trajectory $(x_{\text{switch}}^{\mathcal{T}}, u_{\text{switch}}^{\mathcal{T}})$ with N switches that ends with a state $x_{\text{switch}}^{\mathcal{T}}(t)$ in a ε_1 -neighbourhood of $\tilde{x}(t)$. Notice that N is necessarily finite since there is a non-zero minimum time interval between the switches (N is also bounded, since t is bounded).

Let t_N be a time instant of the last switch. Due to continuity of the LQR tracking trajectory and domination of the assignment rule, there is an ε_2 -neighbourhood of $\tilde{x}(t_N)$ such that

$$\|(x_{\text{switch}}^{\mathcal{T}}(\tau), u_{\text{switch}}^{\mathcal{T}}(\tau)) - (\tilde{x}(\tau), \tilde{u}(\tau))\| < \varepsilon_1$$

for all $\tau \in [t_N, t]$ regardless of an exact assigned trajectory. We will repeat the argument for the second last switch t_{N-1} and find an ε_3 -neighbourhood of $\tilde{x}(t_{N-1})$ such that

$$\|(x_{\text{switch}}^{\mathcal{T}}(\tau), u_{\text{switch}}^{\mathcal{T}}(\tau)) - (\tilde{x}(\tau), \tilde{u}(\tau))\| < \varepsilon_2$$

for all $\tau \in [t_{N-1}, t_N]$ regardless of an assigned trajectory. In the end, we will find a ε_{N+1} -neighbourhood of $\tilde{x}(0)$ such that

$$\|(x_{\text{switch}}^{\mathcal{T}}(\tau), u_{\text{switch}}^{\mathcal{T}}(\tau)) - (\tilde{x}(\tau), \tilde{u}(\tau))\| < \varepsilon_{N+1}$$

for all $\tau \in [0, t_1]$ and regardless of an assigned trajectory. Hence, we have for a given number of switches and switch instants a neighbourhood $\tilde{x}(0)$ such that

$$\|(x_{\text{switch}}^{\mathcal{T}}(\tau), u_{\text{switch}}^{\mathcal{T}}(\tau)) - (\tilde{x}(\tau), \tilde{u}(\tau))\| < \varepsilon_1 = \max_{i=1, \dots, N+1} \varepsilon_i$$

for all $\tau \in [0, t]$ regardless of all assigned trajectories. Also remember, that ε_1 can be chosen arbitrary small. Hence, the cost the trajectory $(x_{\text{switch}}^{\mathcal{T}}, u_{\text{switch}}^{\mathcal{T}})$ meets due to the proposition before

$$|\text{cost}_{V_i}(x_0, u_{\text{switch}}^{\mathcal{T}}) - \text{cost}_{V_i}(\tilde{x}(0), \tilde{u})| \leq C t \varepsilon_1$$

and we can consequently make the difference in cost for any given switching scheme arbitrarily small and that concludes the proof. \square

A.2 Proof of Stability

We now prove that the LQR switching control law $u_{\text{switch}}^{\mathcal{T}}$ that is sufficiently decreasing wrt. a suitable Lyapunov function L reaches given ε_0 -neighbourhood around the equilibrium.

Proposition 4. *Let $L : D \rightarrow \mathbb{R}$ be continuously differentiable, positive on $D \setminus H^{\varepsilon_0}$ and compatible with a set of demonstrations \mathcal{T} . Then any system trajectory wrt. an LQR switching control law that is sufficiently decreasing wrt. L stays in S , and visits H^{ε_0} after finitely many trajectory switches.*

Proof. Let $(x_{\text{switch}}^{\mathcal{T}}, u_{\text{switch}}^{\mathcal{T}})$ be a system trajectory with $u_{\text{switch}}^{\mathcal{T}}$ controller and let $x_{\text{switch}}^{\mathcal{T}}(0) \equiv x_0 \in D \setminus H^{\varepsilon_0}$ be an initial state. Let $\tilde{x}_0(0)$ be a start of an assigned trajectory $(\tilde{x}_0, \tilde{u}_0)$. According to Definition 5, there exists the time instant $t_0 > 0$ and the corresponding state $x_{\text{switch}}^{\mathcal{T}}(t_0) \equiv x_1$ such that trajectory switch happened. In such time, $(x_{\text{switch}}^{\mathcal{T}}(t), u_{\text{switch}}^{\mathcal{T}}(t)) \in S$ for all $t \in [0, t_0]$, $x_1 \in \overset{\circ}{D}$ and

$$L(x_1) - L(x_0) \leq \gamma [L(\tilde{x}_0(t_0)) - L(\tilde{x}_0(0))].$$

The norm of the state x_1 is either lesser than ε_0 (we are done) or not. Assume the latter and assume that the a new assigned target trajectory is $(\tilde{x}_1, \tilde{u}_1)$. We control the system according to this trajectory until we hit the time $t_1 + t_0$ and the state x_2 and so on. As a whole, we get a sequence of visited states $(x_i)_{i=0,1,2,\dots}$ contained in D , a sequence of trajectory starts $(\tilde{x}_i(0))_{i=0,1,2,\dots}$, and a sequence of trajectory ends $(\tilde{x}_i(t_i))_{i=0,1,2,\dots}$ such that

$$L(x_{i+1}) - L(x_i) \leq \gamma [L(\tilde{x}_i(t_i)) - L(\tilde{x}_i(0))].$$

Since $L(x)$ is compatible with \mathcal{T} , necessarily $L(\tilde{x}(t)) - L(\tilde{x}(0)) < 0$ for any initial state $\tilde{x}(0)$ of any trajectory in \mathcal{T} and any time $t > 0$. Moreover, we know that $L(\tilde{x}(t))$ decreases monotonically and hence $L(\tilde{x}(t)) - L(\tilde{x}(0)) < L(\tilde{x}(t_{\min})) - L(\tilde{x}(0))$ for any $t > t_{\min}$, where $t_{\min} > 0$ is a minimum switching time used for construction of $(x_{\text{switch}}^{\mathcal{T}}, u_{\text{switch}}^{\mathcal{T}})$.

We let (we denote a set of all initial states as \mathcal{T}_0)

$$0 > C = \max_{\tilde{x}(0) \in \mathcal{T}_0} L(\tilde{x}(t_{\min})) - L(\tilde{x}(0)). \quad (27)$$

The value C is properly defined, since $\tilde{x}(t_{\min})$ as a function of $\tilde{x}(0)$ continuous due to our assumptions on continuity of demonstrations, see Definition 1.

Since $C < 0$,

$$\gamma [L(\tilde{x}(t)) - L(\tilde{x}(0))] \leq \gamma C < 0$$

for any $\tilde{x}(0) \in \mathcal{T}_0$ and thus

$$L(x_{i+1}) - L(x_i) \leq \gamma [L(\tilde{x}_i(t_i)) - L(\tilde{x}_i(0))] \leq \gamma C < 0$$

for all $i = 0, 1, 2, \dots$. In other words, the value of $L(x)$ decreases in every step of the sequence at least by γC . Since $L(x) > 0$ on $D \setminus H^{\varepsilon_0}$, some state in the sequence must be in H^{ε_0} after finitely many switches and thus is the proof concluded. \square

A.3 Proofs of Properties of Algorithms 2 and 3

We assume a demonstrator that provides continuous demonstrations of length T that meet Definition 1 and that are continuous wrt. to their initial states. We are also given a Lyapunov function L that is compatible with this demonstrator. We choose an assignment rule ϕ that is dominated by Euclidean norm, and we choose parameters $\gamma = 0$, $t_{\min} > 0$. Then the following holds.

Proposition 5. *Algorithm 2 provides a stabilizing control law in finitely many iterations.*

Proof. Essentially, our goal is to show that the algorithm produces such set of trajectories that $u_{\text{switch}}^{\mathcal{T}}$ is sufficiently decreasing wrt. L . To do that, we use the fact that LQR tracking trajectories $\Sigma(x_0, u_{\text{LQR}}^{(\tilde{x}, \tilde{u})})$ are uniformly continuous thanks to Proposition 1 together with the fact that our assignment rule is strongly equivalent with the Euclidean norm.

These facts together with an observation, that all demonstrations necessarily visits $\overset{\circ}{D}$ (every demonstration is continuous, is of length T , and must end in H^{ϵ_0}) imply that there is $\tilde{\epsilon} > 0$ such that every LQR tracking trajectory with an initial point x_0 in the $\tilde{\epsilon}$ -neighbourhood around any initial point of any demonstration $\tilde{x}(0)$ meet condition (5) of a sufficient decrease of L for some state in $\overset{\circ}{D}$. Since Algorithm 2 adds new trajectory when the decrease condition is not met, Algorithm 2 can add during its run only finitely many trajectories, since $D \setminus H^{\epsilon_0}$ is compact.

We now show that all points meet condition (5) after finitely many iterations. Let us derive it via the contradiction. Let us assume an iteration, where last trajectory was added. Assume that there is a point that does not meet condition (5) (we will assume that condition is not met strictly since the boundary cases still imply stabilization). Then again due to continuity of $\Sigma(x_0, u_{\text{LQR}}^{(\tilde{x}, \tilde{u})})$, there is a whole neighbourhood around this counterexample that does not meet condition (5) as well. But we sample the state space densely and dense sampling minus finitely many points is still dense. Consequently, the algorithm will sample this neighbourhood eventually and must add another trajectory. But that is a contradiction with the fact that we investigated the run of the algorithm after all trajectories were added.

Hence, all points meet condition (5), which implies that $u_{\text{switch}}^{\mathcal{T}}$ is sufficiently decreasing wrt. L . This fact together with Corollary (1) finishes the proof. \square

If a suitable Lyapunov function L is not known, Algorithm 3 learns one or fails.

Proposition 6. *Algorithm 3 either fails or provides a stabilizing control law in finitely many iterations.*

Proof. We showed in the Section 4.3.2 that a number of changes of candidates $L_p(x)$ is finite. Thus, we can find a maximum iteration of the algorithm, when the last change occurs. In this iteration, the algorithm either ends with failure (since the volume of the set admissible parameters is less than tolerance) or proceeds successfully with the latest candidate $L(x, p)$. This candidate is compatible with all trajectories in \mathcal{T} generated during the whole run of the algorithm.

Thus, the rest of the run is de facto the same as in Algorithm 2 and the set of all remaining samples is still dense since we again possibly lost only finitely many samples. The rest of the argumentation is the same as in the proof of Proposition 5. \square